11-2015

Hornbrook Formation, Oregon and California: A Sedimentary Record of the Late Cretaceous Sierran Magmatic Flare-Up Event

Kathleen D. Surpless
Trinity University, ksurples@trinity.edu

Research Paper

GEOSPHERE

GEOSPHERE; v. 11, no. 6

doi:10.1130/GES01186.1

11 figures; 1 table; 2 supplemental files

CORRESPONDENCE: ksurples@trinity.edu

CITATION: Surpless, K.D., 2015, Hornbrook Formation, Oregon and California: A sedimentary record of the Late Cretaceous Sierran magmatic flare-up event: Geosphere, v. 11, no. 6, p. 1770–1789, doi:10.1130/GES01186.1.

Received 9 March 2015
Revision received 18 August 2015
Accepted 22 September 2015
Published online 10 November 2015

Hornbrook Formation, Oregon and California: A sedimentary record of the Late Cretaceous Sierran magmatic flare-up event

Kathleen D. Surpless

Department of Geosciences, Trinity University, One Trinity Place, San Antonio, Texas 78212, USA

ABSTRACT

Early Late Cretaceous time was characterized by a major magmatic flare-up event in the Sierra Nevada batholith and early phases of magmatism in the Idaho batholith, but the sedimentary record of this voluminous magmatism in the U.S. Cordillera is considerably less conspicuous. New detrital zircon U-Pb ages from the Hornbrook Formation in southern Oregon and northern California reveal a significant and sustained influx of 100–85 Ma detrital zircons into the broader Hornbrook region beginning ca. 90 Ma. Detrital zircon ages and hafnium isotopic compositions, combined with whole-rock geochemistry, suggest that sediment was largely derived from the Sierra Nevada, requiring uplift and erosion of the Sierra Nevada batholith during and immediately following the Late Cretaceous magmatic flare-up event. Sediment derived from the eroded arc may have been transported northward along the axis of the arc, between a western drainage divide along the arc crest and the rising Nevadaplano to the east. Although the Klamath Mountains and Blue Mountains Province present more proximal potential sources of Jurassic and Early Cretaceous detrital zircons in the Hornbrook Formation than the Sierra Nevada, Late Cretaceous deposition on the Klamath Mountains 80 km west of Hornbrook Formation outcrops, and Late Cretaceous deep-water deposition on the Blue Mountains in the Ochoco Basin suggest that these regions were the locus of subsidence and sedimentation, rather than erosion, during Late Cretaceous time. The limited outcrop extent of the Hornbrook Formation may represent only a sliver of a much larger Late Cretaceous Hornbrook basin system. Complete characterization of the episodic magmatic history of continental arcs requires integration of age distributions from the arc itself and from detrital zircons eroded from the arc; it is critical to recognize the potential of drainage systems to transport sediment to depocenters not directly linked to present-day arc exposures.

INTRODUCTION

The complex history of Late Cretaceous plate convergence and arc magmatism in the U.S. Cordillera may be deciphered from the eroded remnants of Cordilleran arcs exposed at the surface today, as well as from basins that received sediment eroded from magmatic arcs and associated terranes (e.g., Barth et al., 2013; Gehrels, 2014). The batholiths that comprise the bulk of continental magmatic arcs form incrementally through long-term magmatism that is episodically punctuated by short-term, high-volume magmatic flare-ups (e.g., Ducea, 2001; de Silva et al., 2015; Ducea et al., 2015; Paterson and Ducea, 2015). A key to the accurate interpretation of the episodic magmatic history of continental arcs is the integration of age distributions from the arc itself and from detrital zircons eroded from the arc that are typically archived in forearc, intra-arc, and backarc basins (e.g., Gehrels, 2014; Ducea et al., 2015; Paterson and Ducea, 2015).

The first 15 m.y. of Late Cretaceous time was characterized by a significant magmatic flare-up event in the Sierra Nevada (Coleman and Glazner, 1997; Ducea, 2001; Ducea and Barton, 2007; Cao et al., 2015) that reached spatial addition rates of up to 1000 km²/km/m.y. (Paterson et al., 2011) and accounted for nearly 78% of the California arc magmatic volume (Ducea, 2001). Magma addition to the Sierran arc during the Late Cretaceous flare-up was 100–1000 times greater than during the preceding magmatic lull, and the vast majority of that magma crystallized at depth, resulting in a plutonic to volcanic ratio of 30:1 or greater (Paterson and Ducea, 2015). In addition, the first phase of magmatism in the Idaho batholith occurred ca. 98–87 Ma, and although these rocks are now exposed only as outlying stocks and roof pendants, they may have originally formed an extensive and continuous igneous complex at a higher structural level than current exposure (Gaschnig et al., 2010, 2011).

Given the ubiquity of zircon in silicic igneous rocks (e.g., Gehrels, 2012) and exhumation of the plutonic system beginning ca. 90 Ma (e.g., Cecil et al., 2006; Giorgis et al., 2008), the sedimentary record of this Late Cretaceous magmatism is surprisingly sparse. Detrital zircons of 100–85 Ma age are more abundant in the retroarc than the forearc regions of the California-Oregon segment of the Cordillera, but they do not dominate the retroarc detrital zircon age signature (Barth et al., 2004; Dickinson and Gehrels, 2008; Dickinson et al., 2012), and they form only a minor component of the Cenomanian–Coniacian (ca. 100–86 Ma) Great Valley forearc basin (DeGraaff-Surpless et al., 2002; Sharman et al., 2015). Although 100–85 Ma detrital zircons are more abundant in Santonian and younger forearc strata of the Great Valley forearc (deposited after ca. 86 Ma), they are typically part of a broader spectrum of Mesozoic grains, likely reflecting expanding catchments rather than deeper erosion of the Late Cretaceous plutons (DeGraaff-Surpless et al., 2002; Sharman et al., 2015).

This study presents new detrital zircon U-Pb ages from the Hornbrook Formation in southern Oregon and northern California, as well as from coeval sedimentary rocks deposited on Klamath Mountains' basement near the southern Oregon town of Cave Junction (Figs. 1 and 2). These new data are integrated with detrital zircon hafnium isotopic data, and whole-rock major- and trace-

element geochemical data from Hornbrook Formation sandstone, siltstone, and mudstone samples. The results document a significant and sustained influx of 100–85 Ma detrital zircon into the broader Hornbrook region beginning at ca. 90 Ma and continuing for at least 10 m.y., into Campanian time. Detrital zircon ages and hafnium isotopic composition and whole-rock geochemistry results suggest that this sediment was largely derived from the Sierra Nevada, although a portion may have been from the early phase of the Idaho batholith. Thus, Sierran-derived sediment may have been funneled northward and westward into the Hornbrook basin beginning ca. 90 Ma, suggesting increased uplift and erosion of the Late Cretaceous Sierra Nevada batholith during and immediately following the Late Cretaceous magmatic flare-up event.

Uplift of the Nevadaplano (e.g., DeCelles, 2004) and Sierra Nevada (e.g., Cecil et al., 2006), combined with a Cretaceous drainage divide within the Sierra Nevada that precluded west-directed transport of eastern Sierran sediment into the Great Valley forearc basin (e.g., Sharman et al., 2015), may have resulted in the northward transport of abundant Sierran arc detritus into the subsiding Hornbrook region during Late Cretaceous time. These results underscore the potential of intra-arc drainage systems to transport sediment to depocenters not directly linked to present-day arc exposures; these transport pathways are critical to recognize if the detrital zircon record is to provide an integrated, long-term history of magmatic activity.

GEOLOGIC SETTING

The Hornbrook Formation crops out in two northwest-trending belts within the Bear Creek valley in southern Oregon and the Cottonwood Creek valley in northern California (Fig. 2A). The strata unconformably rest on Klamath Mountains basement terranes and are overlain by Paleogene sedimentary and volcanic rocks of the Cascade Range (McKnight, 1971). The Hornbrook Formation is considered a forearc basin (e.g., Nilsen, 1984; Miller et al., 1992), with sediment sources during Albian–Turonian time (ca. 113–90 Ma; Fig. 2C) in the accreted terranes and plutons of the Klamath Mountains and the Sierra Nevada Foothills metamorphic belt, as well as possible sources in northern Nevada (Surpless and Beverly, 2013). Hornbrook sediment sources also included Late Cretaceous plutons of the Sierran batholith and/or early phases of the Idaho batholith during Turonian–Maastrichtian time (ca. 90–66 Ma; Surpless and Beverly, 2013). Sandstone samples are quartzofeldspathic with minor volcanic lithic fragments, and they plot in recycled orogen and dissected arc provenance fields on quartz-feldspar-lithic ternary diagrams of Dickinson et al. (1983; Golia and Nilsen, 1984; Surpless and Beverly, 2013). These sandstone compositions suggest that volcanic sources provided little sediment, and therefore that the detrital zircon in the Hornbrook sandstone was derived largely from plutonic and metamorphic sources.

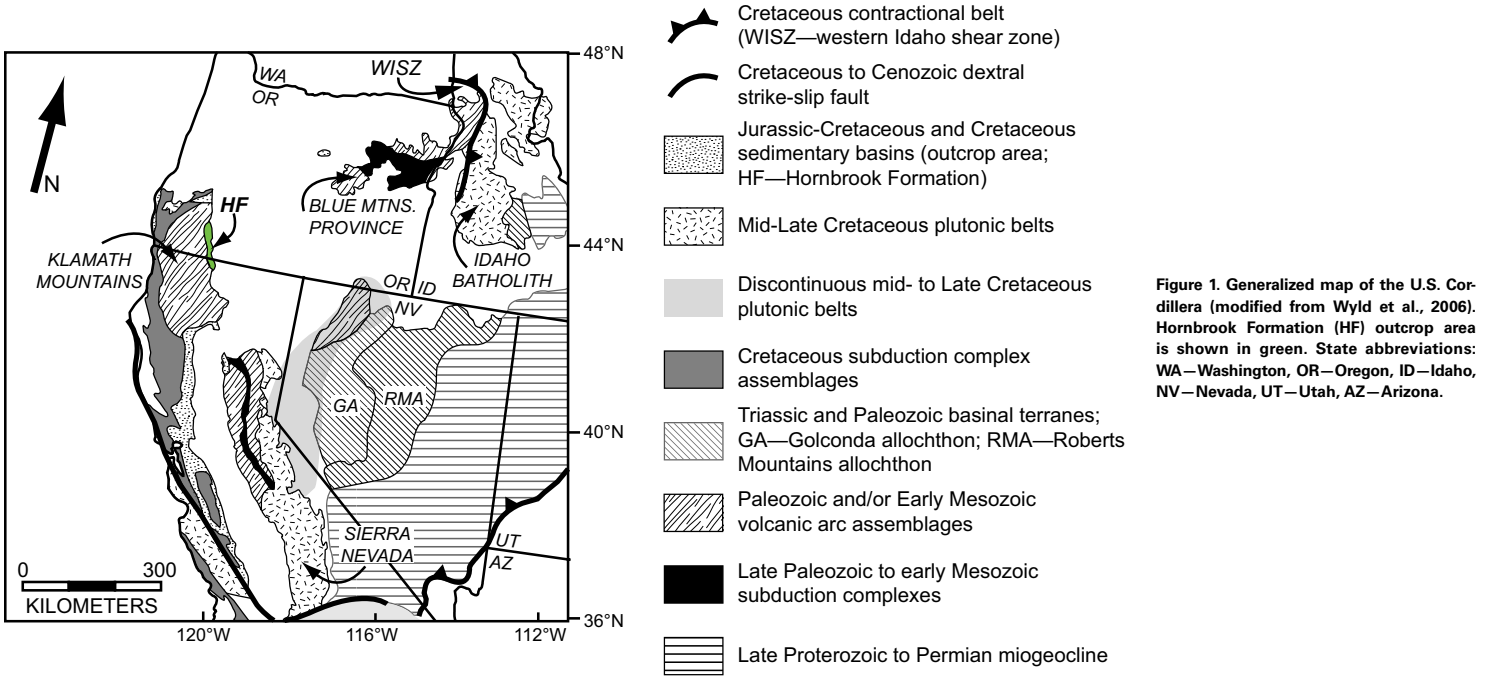

Figure 1. Generalized map of the U.S. Cordillera (modified from Wyld et al., 2006). Hornbrook Formation (HF) outcrop area is shown in green. State abbreviations: WA—Washington, OR—Oregon, ID—Idaho, NV—Nevada, UT—Utah, AZ—Arizona.

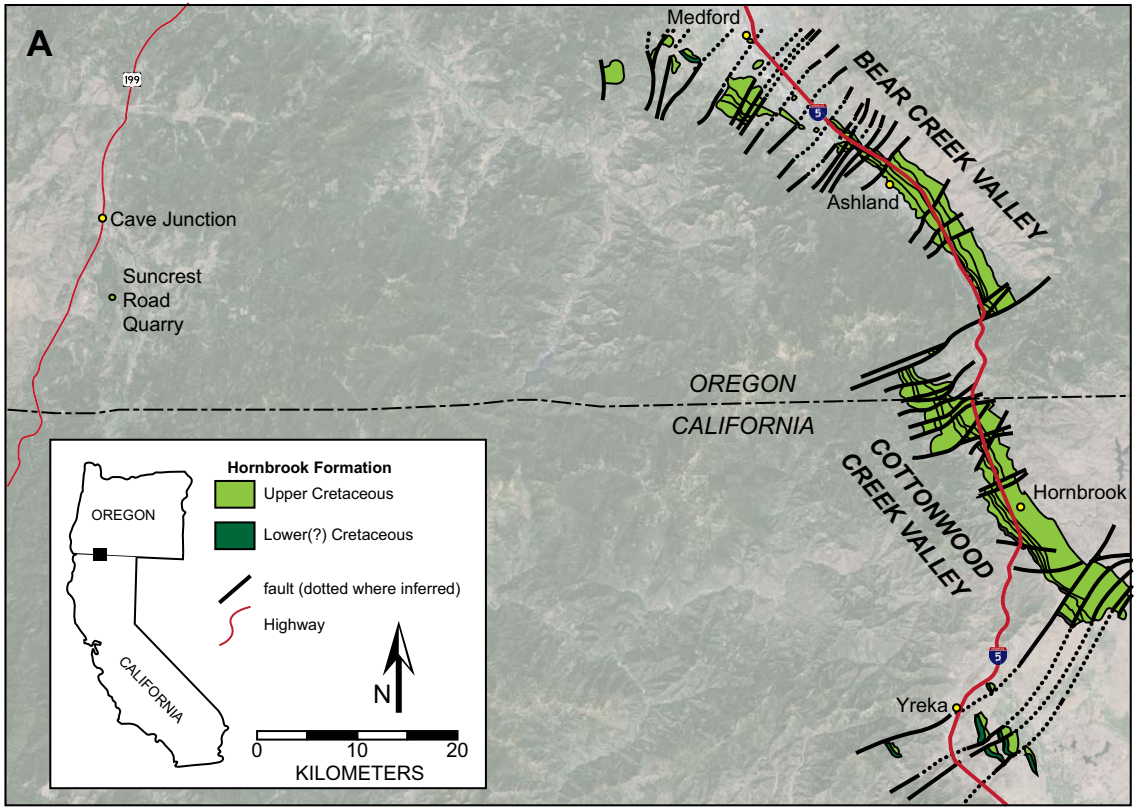

B Hornbrook Formation Members — Depositional Ages

Blue Gulch Mudstone (BGM)		*Campanian–Maastrichtian*
Rocky Gulch Sandstone (RGS)		*Campanian(?)*
Ditch Creek Siltstone (DCS)		*upper Turonian–lower Coniacian(?)*
Osburger Gulch Sandstone (OGS)		*Turonian–lower Coniacian*
	Barneburg Hill (BH)	*middle Turonian(?)*
	Medford Mudstone	*middle Turonian*
	Pioneer Road Sandstone	*middle Turonian*
	Dark Hollow Siltstone	*lower to middle Turonian*
	Ashland Sandstone	*lower to middle Turonian*
Klamath River Conglomerate (KRC)	Jacksonville	*upper (?) Albian to middle Cenomanian*

Bear Creek valley members named by Wiley et al. (2011)

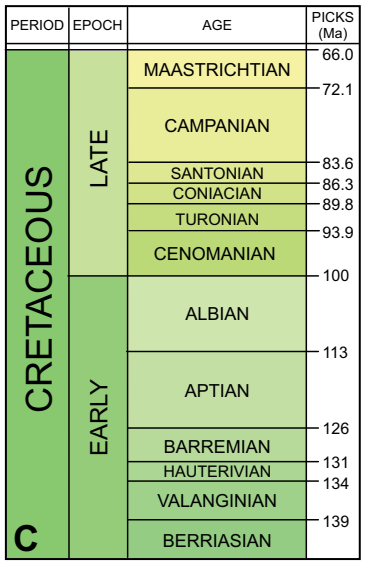

Figure 2. (A) Simplified geologic map of the Hornbrook Formation (from Nilsen, 1993) showing the distribution of outcrop in the Bear Creek and Cottonwood Creek valleys and the location of the Suncrest Road Quarry near Cave Junction, Oregon. Topographic image from Google Earth. (B) Hornbrook Formation member names and depositional ages from Nilsen (1984); proposed new members and depositional ages for the Bear Creek valley from Wiley et al. (2011). (C) Geologic time scale with age names and boundary age picks (Ma) for the Cretaceous Period (from Walker et al., 2012).

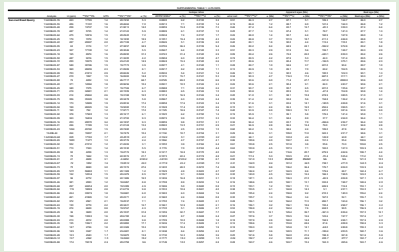

[1]Supplemental Table 1. U-Pb data. Please visit http://dx.doi.org/10.1130/GES01186.S1 or the full-text article on www.gsapubs.org to view Supplemental Table 1.

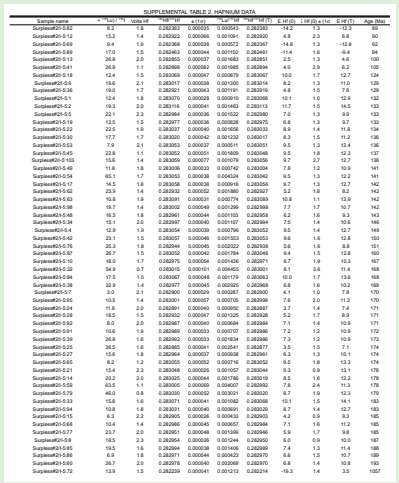

[2]Supplemental Table 2. Hafnium data. Please visit http://dx.doi.org/10.1130/GES01186.S2 or the full-text article on www.gsapubs.org to view Supplemental Table 2.

Hornbrook Formation strata record an overall marine transgression, with fluvial and alluvial deposition at the base of the section and slope and deep basin plain in the middle and upper sections (McKnight, 1971; Elliott, 1971; Nilsen, 1984, 1993). Building on previous work (Peck et al., 1956; Jones, 1959; McKnight, 1971; Elliott, 1971), Nilsen (1984) recognized five members of the Hornbrook Formation (Fig. 2B): (1) the basal Klamath River Conglomerate member formed in fluvial and alluvial depositional environments, with deposition beginning as early as late Albian time (ca. 102 Ma) in the north (Nilsen, 1993) and middle Cenomanian time (ca. 95 Ma) to the south (Jameossanaie and Lindsley-Griffin, 1993); (2) the late Albian–early Coniacian (ca. 102–87 Ma) Osburger Gulch Sandstone member formed in nearshore to wave-dominated middle-shelf environments; (3) the Turonian–Coniacian, ca. 94–86 Ma, Ditch Creek Siltstone member formed in outer-shelf environments; (4) the Rocky Gulch Sandstone member of uncertain age formed in a slope environment, and it unconformably overlies the Ditch Creek Siltstone in the type section; and (5) the Campanian–Maastrichtian (ca. 84–66 Ma) Blue Gulch Mudstone member formed in outer-shelf to basin plain environments. Depositional ages are based on macro- and microfossils and suggest time-transgressive deposition, with deposition becoming younger to the south (Nilsen, 1993). Paleocurrent measurements are dominantly north-directed, with considerable scatter to the east and west (Nilsen, 1984).

Wiley et al. (2011) suggested that the Hornbrook Formation within the Bear Creek valley represents four transgressive sequences separated by three possible unconformities, and they proposed six new members within the basal upper Albian–middle Turonian section of Bear Creek valley that replace, in part, Nilsen's (1984) Klamath River Conglomerate member (Fig. 2B). Only the middle Turonian(?) Barneburg Hill member, which was formerly mapped as the lower conglomerate of the Paleogene Payne Cliffs Formation (McKnight, 1971), was sampled in this study.

Cretaceous sedimentary rocks mapped in the southern Klamath Mountains near the town of Cave Junction (Fig. 2A) have variously been considered part of the Great Valley Group (Knoxville Formation; e.g., Mankinen and Irwin, 1982), Myrtle Group (Days Creek Formation; Imlay et al., 1959), and Hornbrook Formation (Batt et al., 2010). Very limited outcrop extent and poor age control make correlation of these Cretaceous outliers difficult, but detrital zircon age signatures obtained here help to constrain depositional age and therefore potential correlations.

DETRITAL ZIRCON AGE DISTRIBUTIONS AND HAFNIUM ISOTOPIC SIGNATURES

Eleven sandstone samples and three quartzite cobbles were collected from the Ditch Creek Siltstone, Rocky Gulch Sandstone, and Barneburg Hill members of the Hornbrook Formation. In addition, one sandstone sample from Cretaceous siliciclastic rocks in the Suncrest Road Quarry in the Klamath Mountains, ~80 km west-southwest of Ashland, Oregon (Fig. 2A), was collected to improve depositional age constraints and resulting potential correlation of this isolated Cretaceous outlier, which rests unconformably on Jurassic rocks of the Galice Formation (Imlay et al., 1959; Walker and McLeod, 1991). Zircons were isolated using standard separation techniques (e.g., Gehrels et al., 2006), and a random subset of zircon grains from each sample was mounted in epoxy and polished. U-Pb dating and Lu-Hf isotopic analysis were completed at the University of Arizona LaserChron Center, following methods described in Gehrels et al. (2006) and Cecil et al. (2011). Following DeGraaff-Surpless et al. (2003), I include grains younger than 600 Ma that plot within 10% of Tera-Wasserburg concordia along a mixing line from the common Pb value ($^{207}Pb/^{206}Pb$ ratio of 0.86; Cumming and Richards, 1975) through the data to concordia. For grains older than 600 Ma, only grains with less than 10% discordance are included in the probability density plots. Ages reported are $^{206}Pb/^{238}U$ ages for grains younger than 900 Ma and $^{207}Pb/^{206}Pb$ ages for grains 900 Ma and older (all U-Pb data are given in Supplemental Table 1[1]). Lu-Hf isotopic compositions were collected from all grains dated in the Ditch Creek Siltstone sample from the Bear Creek valley (I-5 sample) and from all grains younger than 110 Ma in the Ditch Creek Siltstone sample from the Cottonwood Creek valley (Rickety Bridge sample), using laser ablation of the same spot created during U-Pb analysis (all Hf data are given in Supplemental Table 2[2]). These Ditch Creek Siltstone samples were chosen for Hf analysis because detrital zircon age analysis revealed that the Ditch Creek Siltstone records the first occurrence of the prominent Late Cretaceous detrital zircon age peak, which is the focus of this study.

Mesozoic detrital zircon age distributions for all samples (20 samples; 11 from this study and 9 from Surpless and Beverly, 2013) from Bear Creek and Cottonwood Creek valleys are shown in stratigraphic order by members within each valley, and they are aligned between valleys by similar age distributions, such that members in the northern Bear Creek valley are older than the same member in the southern Cottonwood Creek valley (Fig. 3). Also shown is one sample from the Suncrest Road Quarry in the Klamath Mountains. All samples contain a majority of Mesozoic ages, with Paleozoic and Precambrian grains comprising 2%–14% in Bear Creek valley, and 7%–19% in Cottonwood Creek valley. In total, 14 samples from both Bear Creek and Cottonwood Creek valleys contain a significant proportion of mid- to Late Cretaceous detrital zircons (120–85 Ma), with more variable proportions of Jurassic and Early Cretaceous grains (Fig. 3). Only the Klamath River Conglomerate, Osburger Gulch Sandstone, and Bear Creek valley sample of the Ditch Creek Siltstone member lack abundant mid- to Late Cretaceous zircons.

The detrital zircon age distribution of the newly recognized Barneburg Hill member in the Bear Creek valley (Wiley et al., 2011) is nearly identical to that of the Ditch Creek Siltstone member in the Cottonwood Creek valley and the Suncrest Road Quarry sample, and it is very similar to the Rocky Gulch Sandstone sample in the Bear Creek valley. All of these samples are characterized by a dominant Late Cretaceous peak (ca. 90 Ma), few Early Cretaceous grains, and more Middle–Late Jurassic than Early Jurassic grains. Therefore, the Barneburg Hill member is placed stratigraphically above the Ditch Creek Siltstone member within the Bear Creek valley section, although Wiley et al. (2011) con-

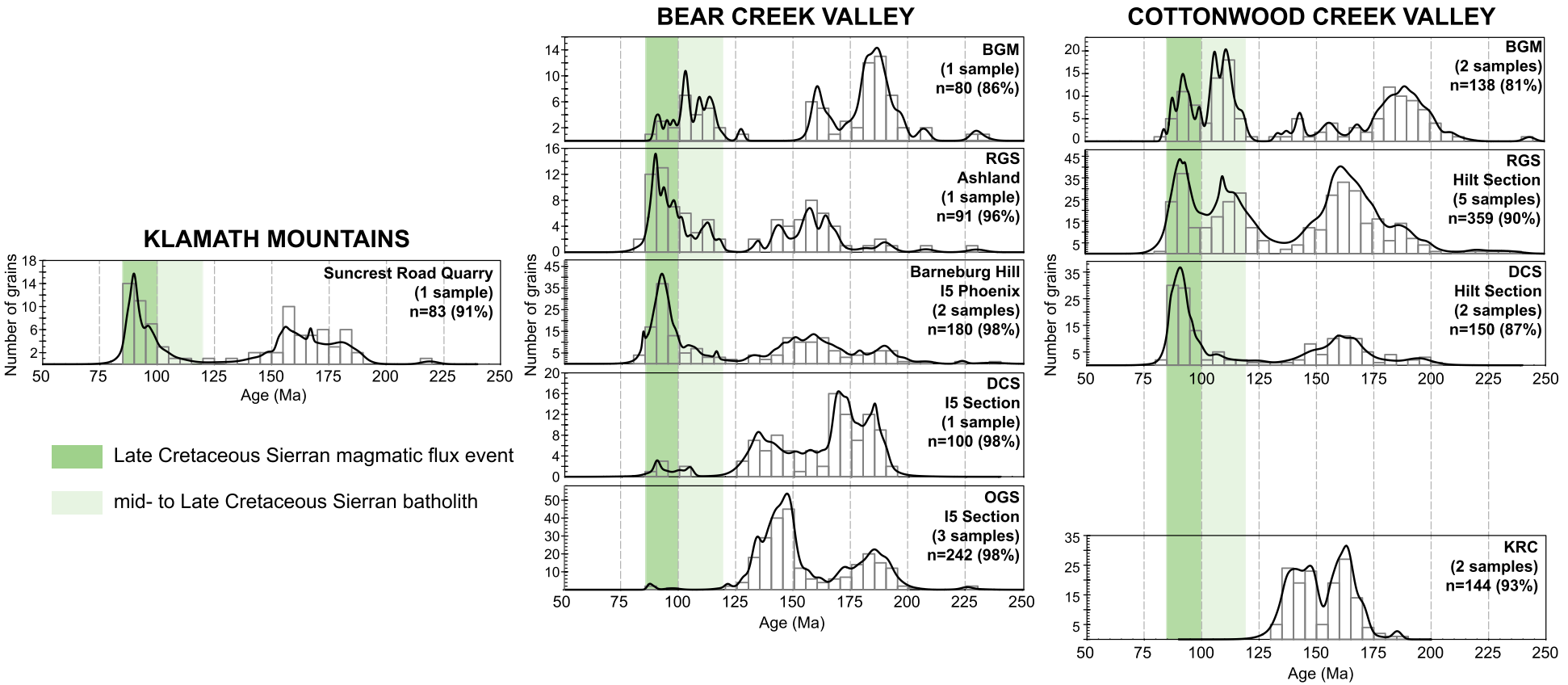

Figure 3. Histograms and superimposed probability density plots of detrital zircon age data for Mesozoic grains in the members of the Hornbrook Formation. Curves are composites of one to five samples from each member, are arranged in stratigraphic order within the Bear Creek and Cottonwood Creek valleys, and are aligned horizontally based on similar depositional age and similar detrital zircon age signatures. Green vertical bars highlight the age of the main Cretaceous batholith of the Sierra Nevada (e.g., Chen and Moore, 1982), with darker-green color indicating the age of the Late Cretaceous magmatic flare-up event in the Sierra Nevada (e.g., Ducea, 2001) and the early phase of magmatism in the Idaho batholith (Gaschnig et al., 2011). Data are from Surpless and Beverly (2013) for Cottonwood Creek valley Klamath River Conglomerate and Blue Gulch Mudstone samples, and for Bear Creek valley Osburger Gulch Sandstone (OGS), Rocky Gulch Sandstone (RGS), and Blue Gulch Mudstone (BGM) samples. DCS—Ditch Creek Siltstone; KRC—Klamath River Conglomerate.

sidered it to be stratigraphically lower than the Ditch Creek Siltstone member and disconformably overlain by the Blue Gulch Mudstone member.

The Mesozoic detrital zircon age distribution of these samples can be subdivided into three groups: (1) a lower group that includes the Klamath River Conglomerate, Osburger Gulch Sandstone, and the Ditch Creek Siltstone in the Bear Creek valley; (2) a middle group that includes the Ditch Creek Siltstone in the Cottonwood Creek valley, Barneburg Hill, and the Suncrest Road Quarry sample; and (3) an upper group that includes the Rocky Gulch Sandstone and Blue Gulch Mudstone (Fig. 4). The lower group contains no Late Cretaceous zircons and variable amounts of Early Jurassic zircons, and it is characterized by an abundance of Middle–Late Jurassic to earliest Cretaceous ages (170–130 Ma). The middle group contains abundant Late Cretaceous zircons with a dominant peak at 92 Ma, few Early Jurassic or Early Cretaceous zircons, and a broad distribution of Middle–Late Jurassic zircons (175–145 Ma). The upper group contains abundant Cretaceous and Jurassic zircons but is more variable than the lower two groups. Very few earliest Cretaceous (140–125 Ma) grains are present in any of these samples.

Paleozoic detrital zircons are present in several samples, but they are limited to a total of only 28 grains ranging from 538 to 252 Ma, with the majority of ages between 370 and 260 Ma (Fig. 5). Precambrian detrital zircons

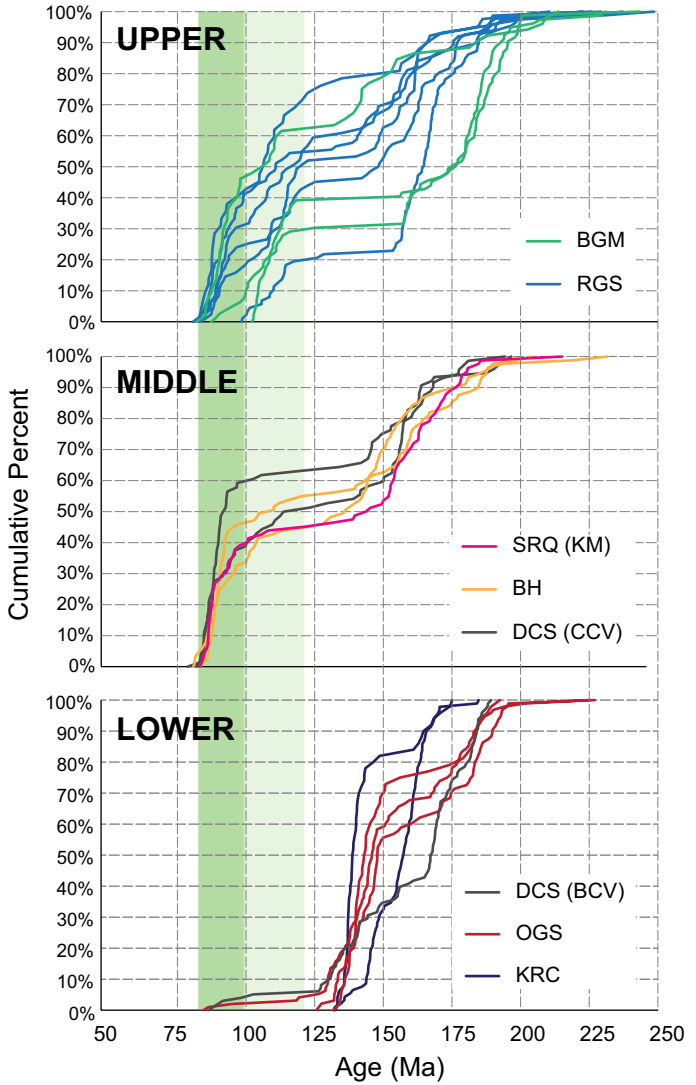

Figure 4. Cumulative probability plots of Mesozoic detrital zircon ages from the Hornbrook Formation, grouped into lower (Klamath River Conglomerate [KRC], Osburger Gulch Sandstone [OGS], and Ditch Creek Siltstone [DCS] in the Bear Creek valley), middle (Ditch Creek Siltstone in Cottonwood Creek valley, Barneburg Hill [BH], and Suncrest Road Quarry [SRQ]), and upper members (Rocky Gulch Sandstone [RGS] and Blue Gulch Mudstone [BGM]) based on depositional age and detrital zircon age signatures; CCV—Cottonwood Creek valley; BCV—Bear Creek valley; KM—Klamath Mountains. Green vertical bars highlight the age of the main Cretaceous batholith of the Sierra Nevada (e.g., Chen and Moore, 1982), with darker-green color indicating the age of the Late Cretaceous magmatic flux event in the Sierra Nevada (e.g., Ducea, 2001) and the early phase of magmatism in the Idaho batholith (Gaschnig et al., 2011).

are more abundant in the Cottonwood Creek valley samples than in the Bear Creek valley samples, comprising up to 19% of any single sample, but they typically constitute less than 10%. Precambrian ages from all Hornbrook sandstone samples have been combined into one distribution (Fig. 6A) that includes two prominent modes ca. 1780 and 1400 Ma, with smaller modes ca. 2470 Ma, 1100 Ma, and 556 Ma, and a spread of grains between 2000 and 1300 Ma. Detrital zircon ages from quartzite cobbles collected from conglomerate units within the Klamath River Conglomerate, Rocky Gulch Sandstone, and Barneburg Hill members have been combined into one distribution (Fig. 6B). Precambrian age modes are similar to those in the sandstone samples, but with only one prominent mode spanning 1850–1700 Ma, smaller modes at ca. 1446 Ma, 1108 Ma, and 668 Ma, and several Late Archean–Paleoproterozoic grains spanning 2900–2400 Ma.

Lu-Hf isotopic analysis of selected Jurassic and Cretaceous grains from Rocky Gulch Sandstone, Ditch Creek Siltstone, Osburger Gulch Sandstone, and Klamath River Conglomerate samples yielded positive, isotopically juvenile ε_{Hf} values of +16 to +5 for all Jurassic and Early Cretaceous grains, and a larger spread of ε_{Hf} values from +13 to –17 for Late Cretaceous grains (Fig. 7).

WHOLE-ROCK GEOCHEMISTRY

Geochemical analysis can help delineate the effects of weathering and sedimentary sorting as well as characterize provenance composition (e.g., McLennan, 1989; McLennan et al., 1993). In total, 24 mudstone, siltstone, and sandstone samples from the Hornbrook Formation were analyzed by inductively coupled plasma–mass spectrometry (ICP-MS) and X-ray fluorescence (XRF) at Washington State University, following procedures of Knaack et al. (1994) and Johnson et al. (1999); data are presented in Table 1.

Major-Element Geochemistry

Major elements are susceptible to postdepositional mobility resulting from chemical weathering and diagenesis, so the degree of weathering can be estimated using the chemical index of alteration (CIA; Nesbitt and Young, 1982). The CIA is a ratio of the mole proportions of Al_2O_3 over the sum of Al_2O_3, K_2O, Na_2O, and CaO*, where CaO* is calculated by correcting for apatite using values of P_2O_5 following McLennan et al. (1993). If the remaining CaO is less than Na_2O, then this value is used as CaO*; if the remaining CaO is more than Na_2O, then Na_2O is considered equivalent to CaO*. Because weathering generally removes Ca faster than Na, this method to determine CaO* produces minimum CIA values (by up to ~3%; Mongelli et al., 2006). The ratio is multiplied by 100, such that fresh igneous and metamorphic rocks have CIA values of 45–55, shale has CIA values of 65–75, and pure aluminosilicate weathering products, such as kaolinite, have a CIA value of 100 (Taylor and McLennan, 1985; McLennan et al., 1993). Weathering trends depicted on A-CN-K and A-CNK-FM

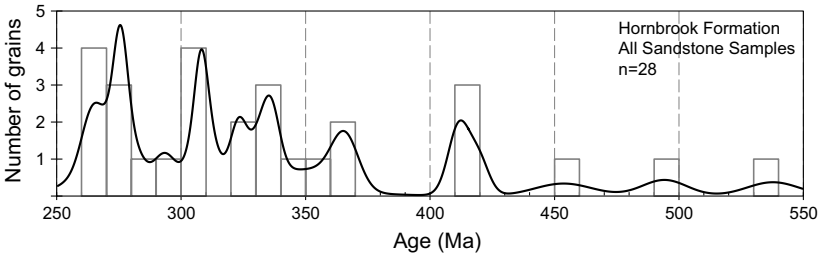

Figure 5. Composite histogram and superimposed probability density plot of all Paleozoic detrital zircon grains from all members of the Hornbrook Formation. Data are from Surpless and Beverly (2013) and this study.

diagrams (where A = Al_2O_3, C = CaO*, N = Na_2O, K = K_2O, F = total Fe as FeO, and M = MgO; after Nesbitt and Young, 1984, 1989) largely result from the conversion of feldspar and glass to clay minerals (McLennan et al., 1990). Mixing provenance components of different weathering histories or compositions, as well as diagenetic reactions involving addition or loss of these elements, will shift samples away from expected weathering trends.

Hornbrook Formation samples separate according to grain size on A-CN-K and A-CNK-FM diagrams (Fig. 8). Sandstone samples have CIA values of 62–67, with an average of 64, suggesting extensive weathering and/or diagenetic alteration, and siltstone and mudstone CIA values range from 71 to 89, with an average value of 77 (Fig. 8A). The finer-grained samples plot largely in the trailing edge (passive margin) tectonic setting for mudstones of McLennan et al. (1990), and sandstone samples plot between the forearc tectonic setting for sands and trailing edge tectonic setting for muds, within a region typified by sands within continental collision, strike-slip, and/or backarc tectonic settings (Fig. 8A; McLennan et al., 1990). Only the Klamath River Conglomerate sample plots along the weathering trend of island-arc andesite; all other samples plot between the weathering trends for island-arc andesite and upper crust on the A-CN-K diagram (Fig. 8A). Hornbrook Formation samples largely plot between weathering trends for andesite and granodiorite compositions on an A-CNK-FM diagram, with a greater spread in apparent source rock compositions in the sandstone samples than the fine-grained samples (Fig. 8B). The lower Hornbrook Formation samples (Klamath River Conglomerate, Osburger Gulch Sandstone, and Ditch Creek Siltstone) appear more intermediate in composition, whereas the upper Hornbrook Formation (Rocky Gulch Sandstone and Blue Gulch Mudstone) straddles the granodiorite weathering trend, and the Blue Gulch Mudstone sandstone samples show the most felsic sources. The higher proportion of Precambrian detrital zircons in the three detrital zircon samples from the Blue Gulch Mudstone (14% and 19%; Fig. 3) suggests an increase in nonarc sediment sources, perhaps contributing to the more felsic geochemical signature of the Blue Gulch Mudstone sandstone samples (Fig. 8). The Hornbrook samples are more extensively weathered and/or altered than samples expected in typical forearc basins, and they include abundant intermediate to felsic source material.

Trace-Element Geochemistry

Trace elements (large ion lithophile elements [LILEs], high field strength elements [HFSEs], and rare earth elements [REEs]) can be powerful provenance indicators because of low postdepositional mobility and exclusion from seawater (McLennan et al., 1993). In addition, immobile trace elements can highlight differences between samples (Ryan and Williams, 2007), revealing changes within basin stratigraphy and between basins.

Comparing incompatible elements Th and Zr against the compatible element Sc provides a measure of the relative importance of magmatic versus sedimentary processes within the source region (e.g., Fralick, 2003). Th/Sc ratio increases with magmatic differentiation, whereas sedimentary recycling concentrates zircon and thereby increases the Zr/Sc ratio (McLennan et al., 1990). A plot of Zr/Sc versus Th/Sc shows enrichment in Zr in all sandstone relative to fine-grained samples, and most samples plot along a trend between andesite and upper-crust granodiorite values, with Blue Gulch Mudstone sandstone clustering around granodiorite values (Fig. 9A; values from Taylor and McLennan, 1985).

A ternary plot of incompatible elements La and Th and compatible element Sc provides another discriminator between juvenile (Sc-enriched) and evolved (La- and Th-enriched) crust (Bhatia and Crook, 1986; McLennan et al., 1990, 1993). Hornbrook samples plot between island-arc andesite and upper continental crust, with lower Hornbrook samples (Klamath River Conglomerate, Osburger Gulch Sandstone, and Ditch Creek Siltstone) plotting closest to island-arc andesite, upper Hornbrook Blue Gulch Mudstone samples closest to North American shale composite (values from Gromet et al., 1984) and upper continental crust, and upper Hornbrook Rocky Gulch Sandstone samples showing the greatest spread (Fig 9B).

A negative europium anomaly is associated with intracrustal differentiation or crystallization of a plagioclase-rich mantle melt that separates plagioclase through partial melting and/or crystal fractionation (e.g., McLennan et al., 1993). The europium anomaly is given as Eu/Eu*, where Eu* is the square root of the product of Sm and Gd concentrations (ppm). Therefore, a plot of Th/Sc versus Eu/Eu* can differentiate different provenance types (Fig. 9C). All but two Hornbrook samples plot within the young differentiated arc field (Eu/Eu* ~0.5–0.9

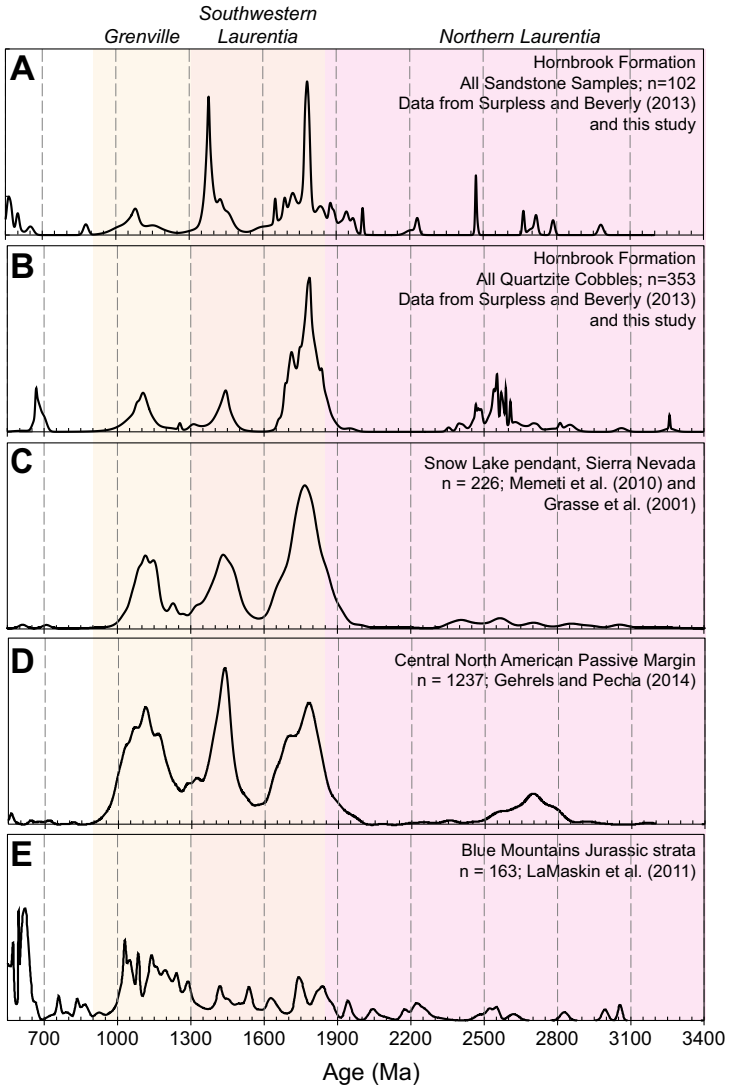

Figure 6. Detrital zircon age signatures for Precambrian grains from the Hornbrook Formation and possible source regions (only grains older than 550 Ma are plotted). Colored vertical shading highlights inferred original crystalline sources of zircon. Plots show composite probability density plots of detrital zircon from: (A) all Hornbrook Formation sandstone samples; (B) Hornbrook Formation quartzite cobbles collected from the Klamath River Conglomerate, Rocky Gulch Sandstone, and Barneburg Hill members; (C) the Snow Lake pendant in the central Sierra Nevada (data from Memeti et al., 2010; Grasse et al., 2001); (D) the Central North American passive margin (Gehrels and Pecha, 2014); and (E) Blue Mountains Jurassic strata (LaMaskin et al., 2011).

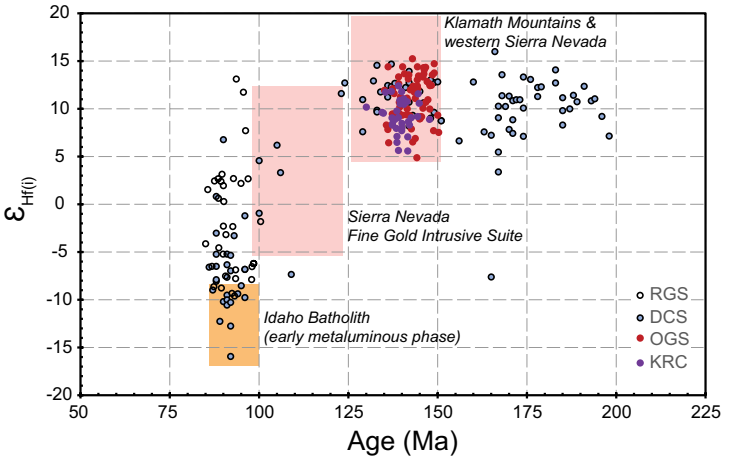

Figure 7. Detrital zircon ε_{Hf} vs. age plot for selected zircon grains from Hornbrook Formation sandstone samples. Data for Klamath River Conglomerate (KRC), Osburger Gulch Sandstone (OGS), and Rocky Gulch Sandstone (RGS) samples are from Surpless and Beverly (2013); data for two Ditch Creek Siltstone (DCS) samples are from this study. Shaded areas represent the range of zircon ε_{Hf} values vs. age for plutons in the Klamath Mountains and western Sierran terranes (Todt et al., 2011), the Fine Gold intrusive suite in the Sierra Nevada (Lackey et al., 2012), and the Idaho batholith (Gaschnig et al., 2011).

and Th/Sc <1; field values from McLennan et al., 1993). Two Blue Gulch Mudstone samples plot within the overlapping old upper continental crust and recycled sedimentary rocks fields (Eu/Eu* ~0.6–0.7 and Th/Sc values = 1; field values from McLennan et al., 1993), consistent with the higher proportion of Precambrian detrital zircon in the Blue Gulch Mudstone (Fig. 3). Chondrite-normalized rare earth element diagrams reveal little variability between Hornbrook samples; all samples show light (L) REE enrichment and intermediate europium anomalies (Fig. 10).

DISCUSSION

Depositional Ages and Stratigraphy

Maximum depositional ages interpreted from the youngest robust detrital zircon ages present in a sample can increase the precision of biostratigraphically determined depositional age ranges and thereby improve estimates of sedimentation rate, provenance changes, and correlation within the Hornbrook Formation. Following Dickinson and Gehrels (2009), the maximum depositional age for Hornbrook Formation samples is estimated by calculating the weighted mean of the youngest three or more grains that overlap at 2σ. In addition, I report the age and uncertainty of the youngest Gaussian age distribution within the sample, as determined by the "Unmix ages" routine in Isoplot version 4.15.11.10.15 (Ludwig, 2011).

TABLE 1. WHOLE-ROCK MAJOR- AND TRACE-ELEMENT GEOCHEMICAL DATA

Member	Klamath River Cgl	Osburger Gulch Sandstone				Ditch Creek Siltstone			Rocky Gulch Sandstone				
Sample:	07-KRC-03	07-OGS-17	07-OGS-14	07-OGS-13	07-OGS-11	07-DCS-16	13-DCS-01	13-DCS-03	07-RGS-30	07-RGS-29	13-RGS-04	13-RGS-05	13-RGS-09
Rock type:	ms	ss	ss	ss	ss	ss	ms	ms	ss	ms	ms	ms	ms
SiO_2 (wt%)	47.59	58.41	61.27	57.76	57.97	61.42	55.03	56.97	63.66	53.45	53.45	55.67	58.41
TiO_2 (wt%)	1.152	0.852	0.860	0.990	1.089	0.829	0.888	0.781	0.565	0.796	0.864	0.822	0.748
Al_2O_3 (wt%)	22.92	14.71	15.33	15.46	14.59	14.36	18.28	17.22	15.00	17.49	19.02	18.32	17.95
FeO* (wt%)	7.03	6.84	6.48	7.00	8.54	5.27	6.86	5.57	4.19	6.40	6.71	6.32	5.63
MnO (wt%)	0.057	0.113	0.095	0.112	0.114	0.096	0.059	0.060	0.052	0.045	0.058	0.053	0.053
MgO (wt%)	2.75	2.54	2.41	2.55	3.36	1.79	3.45	3.38	2.35	3.18	3.69	3.35	2.87
CaO (wt%)	0.91	4.53	2.83	4.57	3.28	3.54	1.84	3.24	2.97	2.06	1.74	1.55	1.26
Na_2O (wt%)	0.53	3.37	3.61	3.29	3.24	2.59	1.32	2.12	3.37	1.17	1.45	1.73	1.84
K_2O (wt%)	1.82	2.20	2.50	2.47	2.31	2.68	2.67	2.81	2.38	3.11	3.35	3.17	3.00
P_2O_5 (wt%)	0.037	0.144	0.125	0.125	0.136	0.101	0.182	0.191	0.172	0.168	0.160	0.162	0.162
Sum (wt%)	84.79	93.71	95.52	94.35	94.63	92.67	90.57	92.35	94.70	87.85	90.48	91.15	91.91
Inductively coupled plasma–mass spectrometry (ICP-MS) data (ppm)													
La	30.02	18.18	17.52	16.46	16.43	15.31	23.20	19.58	24.14	20.18	26.76	17.69	26.94
Ce	62.13	38.95	37.59	35.07	35.79	30.18	46.07	37.64	46.35	34.50	46.92	34.27	52.53
Pr	7.98	5.13	4.90	4.60	4.63	3.62	5.73	4.38	5.53	4.88	6.04	4.17	6.37
Nd	30.80	20.92	20.12	19.15	19.33	14.03	22.38	16.35	20.52	18.96	23.13	16.05	24.48
Sm	6.28	5.02	4.86	4.59	4.62	3.13	4.91	3.37	4.16	4.24	4.75	3.51	5.09
Eu	1.51	1.27	1.26	1.19	1.18	0.80	1.19	0.76	1.03	0.99	1.11	0.90	1.13
Gd	5.08	4.76	4.58	4.45	4.50	2.92	4.38	2.68	3.49	3.93	4.22	3.18	4.56
Tb	0.80	0.79	0.76	0.71	0.73	0.51	0.71	0.42	0.54	0.66	0.67	0.54	0.72
Dy	4.66	4.88	4.60	4.44	4.48	3.15	4.26	2.62	3.18	4.03	4.03	3.49	4.46
Ho	0.88	1.00	0.93	0.90	0.92	0.68	0.86	0.54	0.63	0.85	0.81	0.71	0.89
Er	2.45	2.75	2.58	2.43	2.52	1.89	2.38	1.55	1.69	2.38	2.21	2.09	2.47
Tm	0.37	0.40	0.38	0.36	0.36	0.28	0.36	0.24	0.25	0.36	0.34	0.32	0.37
Yb	2.33	2.60	2.40	2.26	2.32	1.80	2.31	1.62	1.57	2.34	2.27	2.11	2.36
Lu	0.36	0.41	0.39	0.35	0.36	0.29	0.37	0.26	0.25	0.38	0.37	0.34	0.37
Ba	451	589	666	687	592	748	670	714	831	650	705	760	928
Th	9.74	9.08	7.67	5.93	6.68	6.90	7.83	8.52	7.90	7.79	8.62	7.74	9.07
Nb	13.41	7.31	6.85	6.04	6.03	6.64	11.71	12.11	9.83	10.70	12.20	11.23	11.68
Y	20.96	25.01	23.42	22.50	23.23	17.24	21.39	13.17	16.12	21.60	20.87	18.92	22.78
Hf	4.51	8.33	7.35	5.18	5.25	6.13	3.05	3.19	4.11	3.09	3.04	3.01	3.44
Ta	0.92	0.56	0.51	0.46	0.47	0.51	0.83	0.86	0.77	0.73	0.86	0.78	0.83
U	2.00	2.80	2.43	2.02	2.27	2.56	3.19	3.01	3.06	4.61	3.98	3.01	3.41
Pb	10.27	7.28	7.02	7.32	6.99	7.72	20.20	25.47	12.12	19.52	22.80	20.55	21.24
Rb	73.9	61.8	65.9	62.2	53.1	77.0	106.9	109.5	77.4	145.0	134.3	123.4	114.8
Cs	3.95	3.15	3.56	2.33	1.87	3.81	8.29	6.92	2.18	7.07	9.69	7.16	6.20
Sr	115	284	323	305	299	235	142	244	412	355	158	170	168
Sc	33.1	22.7	21.1	19.7	21.6	14.5	22.7	17.3	11.0	21.2	21.3	19.9	18.4
Zr	156	303	265	183	189	219	105	112	146	105	106	104	120
X-ray fluroescence (XRF) data (ppm)													
Cr	227	136	110	89	101	48	89	62	45	95	80	86	76
Ni	170	31	34	25	24	9	51	38	19	50	44	48	41
V	230	219	184	159	173	131	186	148	99	191	183	172	140
Ga	25	16	16	15	16	13	23	22	16	25	25	24	24
Cu	163	34	41	35	34	33	91	61	20	75	93	75	64
Zn	117	80	78	70	71	76	149	128	73	152	146	133	126

(*continued*)

TABLE 1. WHOLE-ROCK MAJOR- AND TRACE-ELEMENT GEOCHEMICAL DATA (*continued*)

Member	Blue Gulch Mudstone										
Sample:	07-BGM-04	07-BGM-05	07-BGM-06	07-BGM-21	07-BGM-250	07-BGM-26	07-BGM-28	07-BGM-22	07-BGM-23	07-BGM-27	13-BGM-01
Rock type:	ss	ss	ss	ss (concretion)	ss	ss	ss	ms	ms	ms	ms
SiO_2 (wt%)	66.41	66.74	67.74	53.93	63.49	59.81	62.04	56.16	56.99	60.43	59.11
TiO_2 (wt%)	0.522	0.510	0.496	0.449	0.643	0.660	0.631	0.797	0.774	0.692	0.745
Al_2O_3 (wt%)	15.11	14.78	14.61	10.53	13.46	12.87	12.47	18.45	18.22	16.30	17.66
FeO* (wt%)	3.90	3.60	3.38	2.60	5.08	4.66	3.92	5.80	5.96	6.73	5.76
MnO (wt%)	0.040	0.038	0.038	0.310	0.110	0.204	0.149	0.060	0.032	0.036	0.054
MgO (wt%)	1.89	1.75	1.56	0.99	1.92	1.83	1.78	2.33	2.29	2.79	2.94
CaO (wt%)	1.54	1.78	1.80	13.44	3.27	6.31	5.63	0.82	0.90	0.82	1.53
Na_2O (wt%)	3.52	3.55	3.75	2.46	2.56	2.37	2.39	1.40	1.36	1.93	1.86
K_2O (wt%)	2.51	2.42	2.37	1.49	1.70	1.92	1.83	2.68	2.65	2.30	2.92
P_2O_5 (wt%)	0.143	0.154	0.156	0.090	0.257	0.178	0.192	0.147	0.206	0.169	0.177
Sum (wt%)	95.59	95.33	95.90	86.29	92.49	90.81	91.03	88.64	89.38	92.19	92.75
Inductively coupled plasma–mass spectrometry (ICP-MS) data (ppm)											
La	26.99	31.58	32.15	15.36	20.34	22.87	23.50	24.45	25.34	21.96	26.81
Ce	53.86	62.74	64.39	29.50	39.83	44.79	47.46	48.54	49.20	42.67	52.53
Pr	6.27	7.31	7.51	3.58	5.04	5.55	6.19	6.08	6.26	5.30	6.35
Nd	23.71	27.64	27.92	13.64	19.66	21.34	25.07	24.06	24.32	20.33	24.06
Sm	4.78	5.53	5.57	2.76	4.32	4.52	5.66	5.32	5.38	4.35	5.02
Eu	1.05	1.14	1.10	0.69	1.21	1.06	1.44	1.32	1.27	1.04	1.11
Gd	4.16	4.69	4.66	2.37	3.97	3.99	5.54	4.73	4.72	3.87	4.33
Tb	0.64	0.73	0.72	0.37	0.65	0.64	0.91	0.78	0.77	0.64	0.69
Dy	3.73	4.28	4.13	2.22	3.82	3.83	5.57	4.82	4.67	3.92	4.20
Ho	0.74	0.85	0.84	0.45	0.80	0.78	1.14	0.98	0.98	0.81	0.83
Er	2.02	2.29	2.24	1.27	2.19	2.17	3.03	2.76	2.76	2.28	2.36
Tm	0.30	0.33	0.33	0.19	0.32	0.32	0.43	0.41	0.42	0.34	0.35
Yb	1.88	2.08	2.10	1.23	2.03	2.04	2.56	2.60	2.63	2.19	2.28
Lu	0.30	0.33	0.33	0.20	0.32	0.33	0.39	0.42	0.43	0.35	0.36
Ba	850	820	887	676	871	857	991	816	864	853	804
Th	7.88	9.28	9.62	4.50	6.39	7.34	6.85	10.25	9.24	7.82	8.79
Nb	9.47	9.51	9.63	4.94	6.77	7.38	7.12	9.00	9.33	8.15	11.75
Y	18.55	21.71	21.49	12.14	21.64	21.04	32.73	25.62	24.90	20.58	21.25
Hf	5.23	6.22	6.26	3.22	4.57	5.67	5.08	3.43	3.62	3.55	3.78
Ta	0.70	0.74	0.75	0.37	0.52	0.57	0.55	0.67	0.67	0.61	0.82
U	2.37	2.58	2.57	1.53	2.53	2.74	2.71	3.40	3.04	2.92	3.24
Pb	12.46	12.06	12.61	6.11	8.92	9.60	10.75	22.56	19.98	16.96	22.91
Rb	84.6	79.4	75.5	42.0	55.0	58.9	59.5	110.3	105.1	90.8	105.5
Cs	2.80	2.55	2.26	1.54	3.07	2.93	3.36	9.90	8.13	6.72	5.97
Sr	328	331	332	260	185	244	243	150	143	155	187
Sc	10.3	9.7	9.7	8.3	13.3	13.7	11.2	18.1	18.2	15.8	17.2
Zr	183	219	221	117	163	204	185	116	123	122	133
X-ray fluroescence (XRF) data (ppm)											
Cr	47	50	47	31	48	50	50	82	79	63	73
Ni	15	13	13	6	17	17	17	39	34	29	41
V	90	86	82	80	120	126	111	196	188	173	136
Ga	17	17	16	10	14	12	13	21	21	17	23
Cu	10	8	8	7	25	21	24	69	69	48	61
Zn	67	63	60	41	75	72	79	158	152	145	132

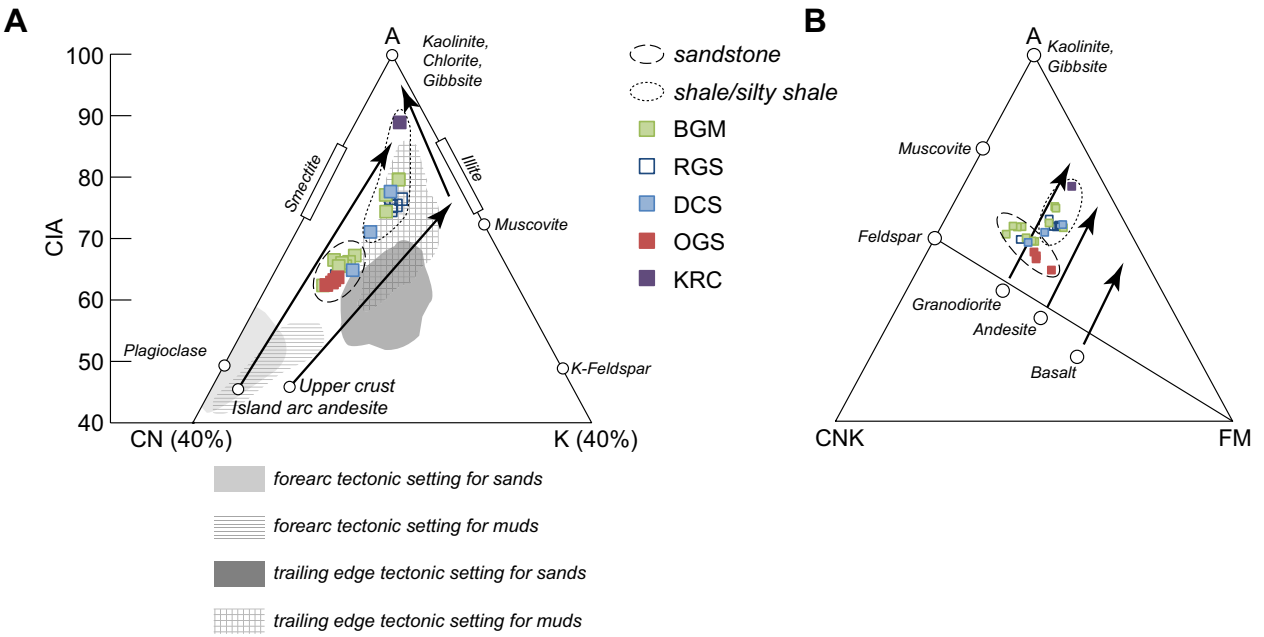

Figure 8. (A) A-CN-K plot vs. chemical index of alteration (CIA), after McLennan et al. (1990), where A—Al_2O_3, CN—CaO (silicate fraction only) + Na_2O, and K—K_2O (after Nesbitt and Young, 1984, 1989). Arrows indicate predicted paths for increasing weathering intensities; Hornbrook Formation samples form a mix between trailing edge and forearc tectonic settings. (B) A-CNK-FM plot after McLennan et al. (1993) where A—Al_2O_3, CNK—CaO (silicate fraction only) + Na_2O + K_2O, and FM—FeO + MgO (after Nesbitt and Young, 1984, 1989). Also plotted are compositions of major minerals and rock types; arrows indicate general weathering trends typical of the various rock types. KRC—Klamath River Conglomerate; OGS—Osburger Gulch Sandstone; DCS—Ditch Creek Siltstone; RGS—Rocky Gulch Sandstone; BGM—Blue Gulch Mudstone.

The Ditch Creek Siltstone member contains pelecypods, gastropods, ammonites, and foraminifera that indicate middle Turonian (92.2–90.5 Ma) deposition in the Bear Creek valley and late Turonian–Coniacian (90.5–86.3 Ma) deposition in the Cottonwood Creek valley (Nilsen, 1993). In the Bear Creek valley, the I-5 sample from the middle of the Ditch Creek Siltstone has a maximum depositional age of 90.5 ± 2 Ma, with the same value resulting from a weighted mean of the youngest four grains and the Unmix routine. Both Ditch Creek Siltstone samples from the Cottonwood Creek valley have maximum depositional ages within Coniacian time: The Rickety Bridge sample from the middle-upper Ditch Creek Siltstone has a maximum depositional age of 87.4 ± 0.9 Ma (n = 15, weighted mean age) or 87.0 ± 1.3 Ma (Unmix), and sample 13-DCS-02 from the upper Ditch Creek Siltstone has a maximum depositional age of 87.2 ± 1.2 Ma (n = 10, weighted mean) or 89.1 ± 0.8 Ma (Unmix). Thus, detrital zircon maximum depositional ages are consistent with time-transgressive deposition in the Ditch Creek Siltstone member.

The proposed Barneburg Hill member of the Bear Creek valley was considered middle Turonian (92.2–90.5 Ma; Wiley et al., 2011) based on foraminifera collected from a site east of Medford (northern Bear Creek valley) that was previously mapped as part of the Rocky Gulch Sandstone member by Nilsen (1984, 1993). Detrital zircon ages presented here are from samples collected south of this locality, within the Barneburg Hill conglomerate, which was previously mapped as the basal conglomerate of the Paleogene Payne Cliffs Formation (McKnight, 1971) and is now considered part of the upper Barneburg Hill member by Wiley et al. (2011). These samples have maximum depositional ages within Turonian–Santonian time (93.9–83.6 Ma). Sample 13-HBF-01 has a late Turonian–early Coniacian maximum depositional age of 89.1 ± 1.6 Ma (n = 9, weighted mean) or 91.3 ± 1.1 Ma (Unmix), whereas sample 08-PC-02 has a Santonian maximum depositional age of 84.5 ± 0.7 Ma (n = 7, weighted mean) or 84.5 ± 0.8 Ma (Unmix). These detrital zircon maximum depositional ages suggest that the Barneburg Hill member at this location is slightly younger than the Turonian Ditch Creek Siltstone member in the Bear Creek valley, and the same age or younger than the Coniacian Ditch Creek Siltstone member in the Cottonwood Creek valley.

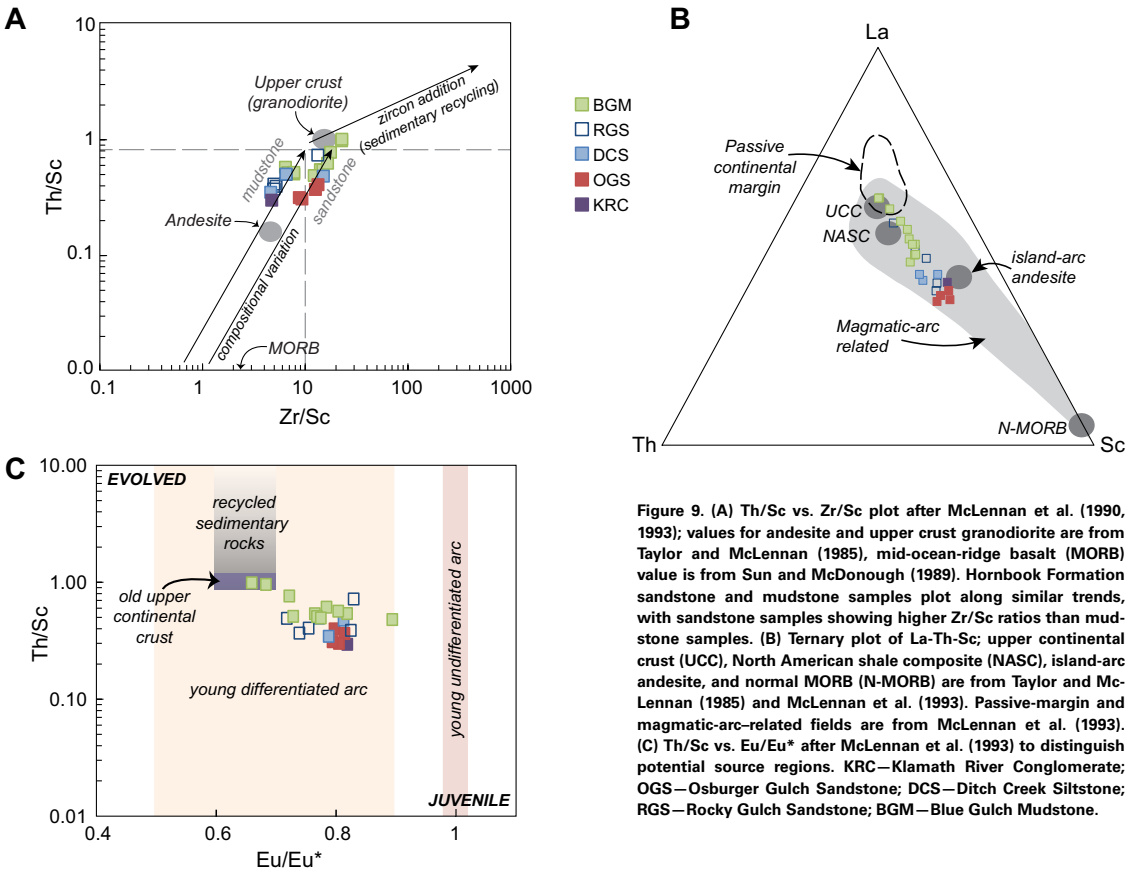

Figure 9. (A) Th/Sc vs. Zr/Sc plot after McLennan et al. (1990, 1993); values for andesite and upper crust granodiorite are from Taylor and McLennan (1985), mid-ocean-ridge basalt (MORB) value is from Sun and McDonough (1989). Hornbrook Formation sandstone and mudstone samples plot along similar trends, with sandstone samples showing higher Zr/Sc ratios than mudstone samples. (B) Ternary plot of La-Th-Sc; upper continental crust (UCC), North American shale composite (NASC), island-arc andesite, and normal MORB (N-MORB) are from Taylor and McLennan (1985) and McLennan et al. (1993). Passive-margin and magmatic-arc–related fields are from McLennan et al. (1993). (C) Th/Sc vs. Eu/Eu* after McLennan et al. (1993) to distinguish potential source regions. KRC—Klamath River Conglomerate; OGS—Osburger Gulch Sandstone; DCS—Ditch Creek Siltstone; RGS—Rocky Gulch Sandstone; BGM—Blue Gulch Mudstone.

Nilsen (1993) reported that the Rocky Gulch Sandstone lacks fossil age control, with the exception of the middle Turonian foraminifera collected from a section east of Medford that Wiley et al. (2011) remapped as part of the Barneburg Hill member. Surpless and Beverly (2013) reported a maximum depositional age of 86 Ma in one Rocky Gulch Sandstone sample from the Bear Creek valley near Ashland. Five detrital zircon samples were collected from a continuous section of the Rocky Gulch Sandstone in the Cottonwood Creek valley; the basal sample, 13-RGS-01, has a maximum depositional age of 89.7 ± 1.3 Ma (n = 11, weighted mean) or 91 ± 1 Ma (Unmix), and the uppermost sample, 13-RGS-08, has a maximum depositional age of 86.3 ± 1.7 Ma (n = 6, weighted mean) or 86.7 ± 2 Ma (Unmix). These ages permit deposition beginning as early as late Turonian and continuing through at least Coniacian time. However, these Rocky Gulch Sandstone samples were collected from a continuous stratigraphic section above 13-DCS-02, which has a Coniacian maximum depositional age, requiring that deposition of the Rocky Gulch Sandstone in the Cottonwood Creek valley began no earlier than Coniacian time (89.8 Ma) and may have extended into Santonian time (beginning 83.6 Ma).

Wiley et al. (2011) noted the presence of a possible middle Coniacian–middle Campanian disconformity between the Ditch Creek Siltstone and the Rocky Gulch Sandstone in the Bear Creek valley, on the basis of the absence of definitive middle–late Coniacian, Santonian, and early–middle Campanian fossil assemblages (Peck et al., 1956; Elliott, 1971), but Nilsen (1993) suggested only local erosion based on his collection of mega- and microfossil ages within that time span. In the Bear Creek valley, detrital zircon ages yield a late Turonian maximum depositional age for the middle Ditch Creek Siltstone member and a Santonian maximum depositional age for the Rocky Gulch Sandstone member, consistent with a possible disconformity between these members (Surpless and Beverly, 2013). However, in the Cottonwood Creek valley, Coniacian maxi-

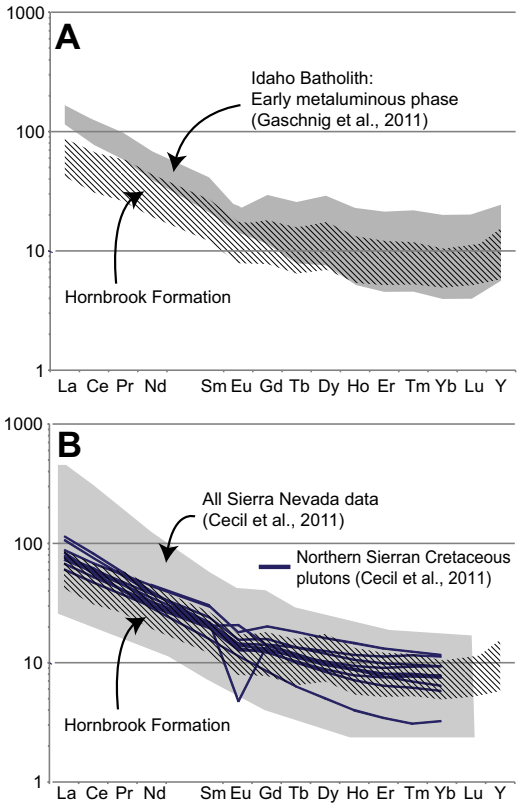

Figure 10. Comparison of chondrite-normalized rare earth element (REE) plots for the Hornbrook Formation (shown in diagonal line pattern) with (A) the early metaluminous phase of the Idaho batholith (data from Gaschnig et al., 2011), and (B) all available REE data from the central and southern Sierra Nevada batholith (light-gray shading; data compiled by Cecil et al. [2012] from the North American volcanic and intrusive rock database [NAVDAT; www.navdat.org]) and Cretaceous plutons of the northern Sierra Nevada (blue lines; data from Cecil et al., 2012). Chondrite values are from Sun and McDonough (1989).

mum depositional ages for both the Ditch Creek Siltstone and the Rocky Gulch Sandstone indicate no major disconformity between these members, suggesting that any Coniacian–Santonian disconformity was not basinwide.

The Suncrest Road Quarry sample collected from the Suncrest Road Quarry ~80 km west-southwest of Ashland, Oregon (Fig. 2A), yields a maximum depositional age of 89.3 ± 0.7 Ma (n = 23, weighted average) or 89.4 ± 0.8 Ma (Unmix). Thus, this Cretaceous outlier in the Klamath Mountains, previously considered part of the Valanginian–Barremian Days Creek Formation of the Myrtle Group (Imlay et al., 1959), was deposited no earlier than Coniacian time and is time-correlative with the Hornbrook Formation.

Taken together, these maximum depositional ages are consistent with time-transgressive deposition of the Hornbrook Formation; deposition occurred first in the Bear Creek valley to the north before deposition in the Cottonwood Creek valley to the south. In addition, these detrital zircon depositional age constraints, combined with biostratigraphic ages, suggest that most Hornbrook Formation deposition took place in Coniacian–Campanian time (89.8–72.1 Ma). However, estimation of sedimentation rates through this period is hampered by the variable thickness of members, time-transgressive deposition, and the possible presence of one or more disconformities within the section.

Sediment Sources

Given that the Hornbrook basin lies inboard of proposed translated terranes associated with the Baja–British Columbia hypothesis (e.g., Cowan et al., 1997), and that the Klamath Mountains were displaced westward in Late Jurassic or Early Cretaceous time (Irwin, 1960; Jones and Irwin, 1971; Constenius et al., 2000; Ernst et al., 2008; Batt et al., 2010; Ernst, 2013), the current configuration between the Sierra Nevada Foothills metamorphic belt and correlative units in the Klamath Mountains was established prior to deposition of the Hornbrook Formation on the eastern Klamath Mountains. Restoring 38° of post-Albian clockwise rotation (Housen and Dorsey, 2002) places the Blue Mountains Province of central and eastern Oregon close to the Hornbrook Formation by 90 Ma (Fig. 11).

Nilsen (1993) and others (summarized in Nilsen, 1984) suggested that Hornbrook Formation sediment was wholly derived from the Klamath Mountains, but detrital zircon U-Pb age and hafnium isotopic compositions led Surpless and Beverly (2013) to suggest that only the lower Hornbrook Formation (Klamath River Conglomerate, Osburger Gulch Sandstone, Ditch Creek Siltstone in Bear Creek valley) could have had solely Klamath Mountains provenance, and that much of the Hornbrook Formation sediment was derived from the Sierra Nevada and northern Nevada, with additional sediment input from the Blue Mountains possible.

The Coniacian and younger members of the Hornbrook Formation, particularly in the middle group (Fig. 4), are characterized by abundant 100–85 Ma detrital zircon with ε_{Hf} values that range from +13 to –17 (Fig. 7). Whole-rock geochemical analysis of these Hornbrook members (Ditch Creek Siltstone, Rocky Gulch Sandstone, and Blue Gulch Mudstone) indicates provenance in the young differentiated arc field, with source-rock average compositions between island-arc andesite and the North American shale composite and upper continental crust (Fig. 9). The Late Cretaceous age range that characterizes most of the Coniacian and younger Hornbrook strata aligns well with a volumetrically significant magmatic flare-up event in the Sierra Nevada batholith and with the early phase of magmatism in the Idaho batholith, but it

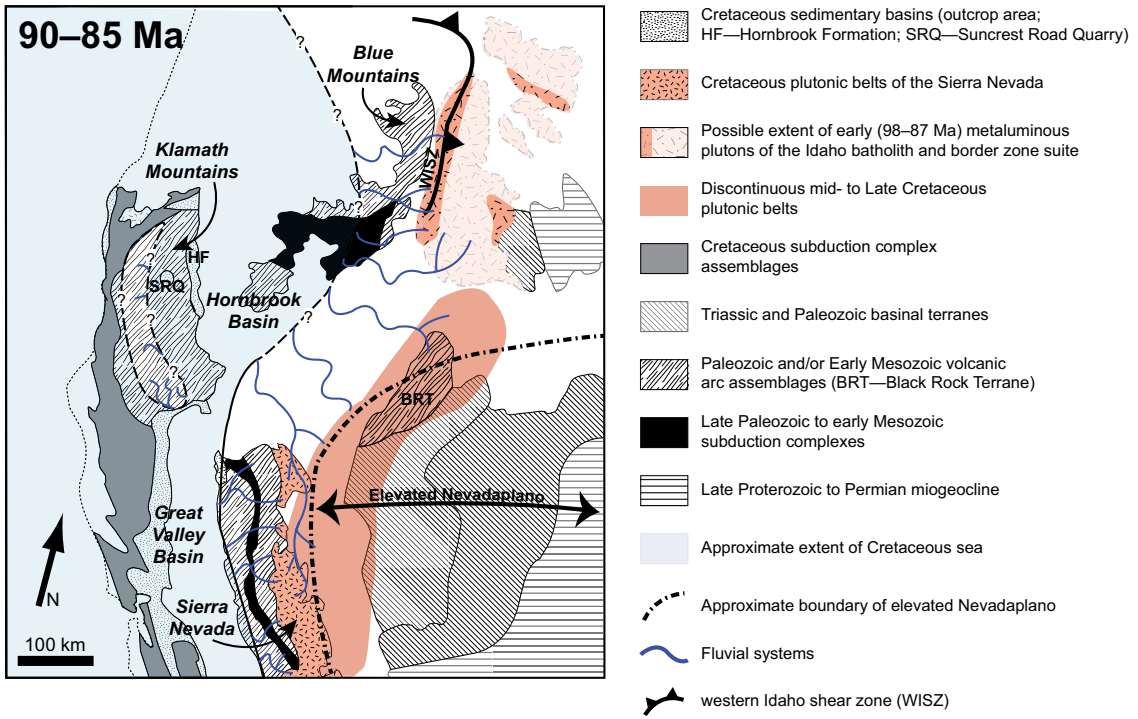

Figure 11. Paleogeographic cartoon for 90–85 Ma showing inferred drainage pathways into the Hornbrook basin region from the south and east. Following Wyld et al.'s (2006) reconstruction, Cenozoic Basin and Range extension, western California strike-slip faulting, and post-Cretaceous rotation of the Blue Mountains have been restored. The extent of Cretaceous Sierran magmatism is based on the paleogeographic map of Van Buer et al. (2009), and the possible extent of Idaho batholith magmatism was estimated based on present mapped exposure of the batholith. Location of the margin of the elevated Nevadaplano is after Sharman et al. (2015), and Cretaceous sea level is after Surpless and Beverly (2013), Sharman et al. (2015), and this study.

does not have a source within the Klamath Mountains or the Blue Mountains. Although they may be nonunique discriminators, ε_{Hf} values and whole-rock geochemical signatures from the Hornbrook strata help differentiate between Late Cretaceous sources entirely within the Idaho batholith, the Sierran arc, or a combination of the two.

Idaho Batholith ± Blue Mountains Source

The Late Cretaceous Idaho batholith is largely younger than 85 Ma, with up to 120 Ma magmatism documented along its western and northwestern margins (Lewis et al., 1987). U-Pb geochronology of the Idaho batholith revealed an early metaluminous suite of plutons that are 98–85 Ma in age (Gaschnig et al., 2011), with ε_{Hf} values that range from –6 to –12 (Gaschnig et al., 2011). These metaluminous plutons occur as outlying stocks and roof pendants within the younger Atlanta lobe (Gaschnig et al., 2011). The 90 Ma border zone suite, immediately east of the western Idaho shear zone, has geochemical and isotopic compositions similar to the early metaluminous phase, leading Gaschnig et al. (2011) to speculate that the two magmatic suites once formed a larger, more continuous igneous complex than modern preservation suggests.

West and southwest of the Late Cretaceous Idaho batholith, the Blue Mountains Province includes Paleozoic and early Mesozoic island-arc and subduction-accretion assemblages that are unconformably overlain by Triassic–Jurassic clastic deposits (Dickinson and Thayer, 1978; Dorsey and LaMaskin, 2007; LaMaskin et al., 2008). The Blue Mountains contain Triassic–Lower Jurassic (238–187 Ma; Northrup et al., 2011), Upper Jurassic (162–150 Ma), and Lower Cretaceous plutons (148–141 Ma and 124–111 Ma; Walker, 1995; Anderson et al., 2011; Schwartz et al., 2011), as well as Triassic and Jurassic clastic strata that contain abundant Precambrian detrital zircons (LaMaskin et al., 2008, 2011). Jurassic strata contain detrital zircon age modes between 500 and 650 Ma and between 1000 and 1300 Ma, with additional ages spanning 1300–2300 Ma, and a few Archean grains (Fig. 6E; LaMaskin et al., 2011). Two 153–150 Ma plutons yielded very positive ε_{Hf} values, ranging from +16 to +10, and four 148–146 Ma plutons have slightly less positive ε_{Hf} values that range from +14 to +4 (Anderson et al., 2011).

Uplift recorded by the western Idaho shear zone from 100 to 90 Ma exhumed midcrustal rocks (e.g., Giorgis et al., 2008; Benford et al., 2010) and

could have led to rapid erosion of a volumetrically significant early metaluminous phase and border zone suite of the Idaho batholith, providing abundant 98–87 Ma detritus to catchments draining the uplifted region. Although the early phase of the Idaho batholith is characterized by a less-evolved isotopic signature than later phases of peraluminous magmatism (Gaschnig et al., 2011), the ε_{Hf} values of the early metaluminous phase range from –6 to –12, overlapping with only the most-evolved Late Cretaceous detrital zircons within the Hornbrook Formation (ε_{Hf} values range from +13 to –16; Fig. 7). Hornbrook whole-rock geochemistry reflects all sources of sediment, not only plutonic sources, and therefore it would not be expected to perfectly match Idaho batholith whole-rock samples, but the mismatch between them is significant: Idaho batholith samples show greater LREE enrichment than Hornbrook Formation samples (Fig. 10), with mean La_N/Yb_N values of 22 ± 12 (Gaschnig et al., 2011), compared with upper Hornbrook mean La_N/Yb_N values of only 8 ± 2. Taken together, these mismatches between Idaho batholith and Hornbrook samples suggest that the Late Cretaceous detrital zircon grains in the Hornbrook Formation were not derived solely from the Idaho batholith. However, it remains possible that at least some of the sediment eroded off the rapidly exhumed early magmatic phase of the Idaho batholith was shed westward and comprises a portion of the Late Cretaceous detritus in the Hornbrook Formation.

Transport across the Blue Mountains Province could then have added older, Early Cretaceous and Jurassic sediment to the Hornbrook basin as fluvial systems traversed west and southwest. The result would be a mix of detritus with Jurassic, Early Cretaceous, and Late Cretaceous ages. The older plutons would contribute detrital zircon with positive ε_{Hf} values ranging from +4 to +16, and the Late Cretaceous detrital zircon would have much more-evolved ε_{Hf} values from –6 to –12. Whole-rock geochemical results would reflect mixing of sediment derived from a young, differentiated arc and from the island arc and continental arcs of the Blue Mountains terranes. However, even a combined Idaho batholith–Blue Mountains source area does not provide the abundant 120–100 Ma late Early Cretaceous detrital zircons that characterize the upper Hornbrook samples, particularly in the Cottonwood Creek valley (Fig. 3). Furthermore, Blue Mountains sources would likely contribute abundant Precambrian detrital zircon, as Jurassic and Triassic clastic cover sequences (e.g., LaMaskin et al., 2008, 2011) would be eroded as well as basement terranes and Mesozoic plutons. Although provenance assessment based on Precambrian ages within active tectonic settings must be viewed cautiously due to dilution of Precambrian signatures by abundant arc-derived grains as well as the likelihood of sedimentary recycling (e.g., LaMaskin et al., 2011), the Precambrian ages that characterize the Blue Mountains strata (Fig. 6E) are a poor match for the Precambrian age signature of the Hornbrook Formation (Figs. 6A and 6B). Further, the presence of isolated Cretaceous sedimentary rocks deposited unconformably on the western Blue Mountains terranes (e.g., Oles and Enlows, 1971; Dickinson, 1979) suggests that at least the western Blue Mountains region underwent subsidence and deposition during the middle to Late Cretaceous Period.

Sierra Nevada Source

The terranes of the Sierra Nevada Foothills metamorphic belt are composed of serpentinized ultramafic rocks, blueschists, chert-argillite-limestone mélange, metasedimentary rocks including deep-water quartzites, phyllite, and chert of the Cambrian–Ordovician Shoo Fly complex, and ophiolites (Miller et al., 1992, and references therein; Snow and Scherer, 2006; Ernst et al., 2008), and they have been correlated with similar terranes in the Klamath Mountains (e.g., Irwin, 2003; Ernst, 2013). Passive-margin deposits preserved in a belt of quartzite-rich metasedimentary roof pendants within the axial Sierra Nevada occur east of the Shoo Fly complex within the Western metamorphic belt and west of Sierran roof pendants of the Roberts Mountain allochthon in the Eastern metamorphic belt (Memeti et al., 2010).

Mesozoic magmatism in the Sierra Nevada arc includes magmatic flare-up events during the Triassic (250–200 Ma), Middle and Late Jurassic (180–145 Ma), and mid-Early to Late Cretaceous (124–76 Ma; Barth et al., 2013; Paterson and Ducea, 2015). The Late Cretaceous flare-up event produced the main Cretaceous batholith (Chen and Moore, 1982; Bateman, 1992; Irwin, 2003) and peaked at 99 Ma (Paterson and Ducea, 2015). The ε_{Nd} values for Sierra Nevada plutonic rocks range from +6.5 to –7.9 (DePaolo, 1981; Cecil et al., 2012), with ε_{Nd} values of northern plutons ranging from +2.7 to –7.5 (Cecil et al., 2012). Lower Cretaceous (ca. 138 Ma) plutons in the Sierra Nevada Foothills arc have positive ε_{Hf} values that range from +7 to +19 (Todt et al., 2011). The ε_{Hf} values in 124–105 Ma zircons from the Fine Gold intrusive suite in the central and western Sierra Nevada batholith range from +6.4 to –4.7, with more negative ε_{Hf} values in younger plutons to the east within the suite (Fig. 7; Lackey et al., 2012). Additional Hf data for younger Sierra Nevada batholith rocks are not yet available, precluding further comparison. However, the wide range in Sierran ε_{Nd} values and the >11 epsilon unit spread in ε_{Hf} values for the Fine Gold intrusive suite suggest that ε_{Hf} values of Late Cretaceous Sierran plutons may also be quite variable. Importantly, the better-characterized ε_{Hf} values from the early phase of the Idaho batholith show an evolved signature with much lower variability than either the Early Cretaceous Fine Gold intrusive suite or the Late Cretaceous detrital zircon in the Hornbrook Formation, suggesting that the Idaho batholith could not be the sole source of the Late Cretaceous zircon in the Hornbrook region.

Plutons in the northern Sierra Nevada intruded episodically in Middle to Late Jurassic and middle Cretaceous time, with Late Cretaceous plutons occurring to the northeast, up to 200 km east of the modern Sierran range crest (Barton et al., 1988; Van Buer and Miller, 2010; Cecil et al., 2012); a potentially significant portion of the Late Cretaceous arc may be buried by younger sediment and volcanic rocks in northern California, northwestern Nevada, and southeastern Oregon (Lerch et al., 2007; Van Buer et al., 2009). Whole-rock geochemistry from plutons of the northern Sierra Nevada show LREE enrichment, with La_N/Yb_N ratios ranging from 5 to 35, consistent with the general pattern for plutons of the greater Sierra Nevada (Cecil et al., 2012). Cretaceous plutons trend north-northeast into Nevada, including the Sahwave batholith in

northwestern Nevada, which has similar geochemistry and zonation pattern as plutons of the greater Sierran batholith (Van Buer and Miller, 2010; Cecil et al., 2012). Thus, the northern Sierra Nevada batholith may be much wider than the 60 km width of the exposed southern Sierra Nevada, reaching more than 180 km width at 40°N latitude (Cecil et al., 2012). Cecil et al. (2012) suggest that the northward widening of the batholith resulted in more rapid eastward migration of Cretaceous magmatism and a more dispersed Late Cretaceous magmatic flare-up event that occurred over a longer period of time in the northern batholith than in the south.

The 100–85 Ma magmatic flare-up event in the Sierra Nevada matches the Late Cretaceous age peak that characterizes the middle and upper Hornbrook Formation, and plutons of the northern Sierra, including northwestern Nevada, could also provide the Jurassic and Early Cretaceous detrital zircons that occur throughout the Hornbrook Formation. Moreover, the variability of ε_{Nd} values in the northern Sierran Nevada is consistent with the range in ε_{Nd} values in the Hornbrook Formation (Surpless and Beverly, 2013). The ε_{Hf} data from the Idaho batholith are a poor match for the wide-ranging ε_{Hf} values from Late Cretaceous detrital zircon in the Hornbrook Formation (Fig. 7), but limited ε_{Hf} data for Sierran plutons preclude making a positive comparison of Sierran and Hornbrook ε_{Hf} data. Although nonunique, whole-rock geochemistry of Hornbrook samples is consistent with Sierran sources, and REE distributions match well with Cretaceous plutons of the northern Sierra (Fig. 10; Cecil et al., 2012).

Detrital zircon geochronology of Neoproterozoic through Triassic central North American passive-margin deposits (Utah and Nevada) yield three main Precambrian age populations of 1000–1200 Ma, 1350–1500 Ma, and 1650–1850 Ma, with additional ages between 2500 and 2900 Ma (Fig. 6D; Gehrels and Pecha, 2014). Metasediments in roof pendants in the central Sierra Nevada record similar Precambrian detrital zircon age ranges, albeit with variable proportions (Fig. 6C; Memeti et al., 2010). This passive-margin Precambrian age signature provides a compelling match for the Hornbrook Precambrian age signatures (Fig. 6), with abundant grains originally derived from southwestern Laurentian sources and likely recycled through Paleozoic and early Mesozoic passive-margin deposits (perhaps entirely within the roof pendants within the central Sierra Nevada) before Late Cretaceous deposition in the Hornbrook basin. These Sierran sources of Precambrian zircon also provide a better match to the Hornbrook age signature than the Precambrian age ranges within Jurassic strata of the Blue Mountains (Fig. 6E). Thus, the northern Sierra Nevada region, combined with possible input from the early phase of the Idaho batholith, represents the most likely source of much of the Coniacian and younger Hornbrook sediment (Fig. 11). This extensive source region includes the Sierra Nevada batholith and possibly the Idaho batholith, and currently exposed as well as now-buried plutons in northwestern Nevada, and it also may have included the Black Rock terrane (Surpless and Beverly, 2013).

The oldest Hornbrook strata (lower group of Fig. 4, including the Klamath River Conglomerate, Osburger Gulch Sandstone, and Ditch Creek Siltstone in Bear Creek valley) may have received locally derived sediment from the Sierran Foothills belt, western Sierran batholith, and Klamath Mountains, given the near-absence of Late Cretaceous detrital zircon and abundance of Jurassic and pre–125 Ma Early Cretaceous detrital zircon with juvenile ε_{Hf} values (Surpless and Beverly, 2013). These samples contain very little pre-Mesozoic detrital zircon (2%–7%; Fig. 3), and they plot near island-arc andesite values in a La-Th-Sc ternary diagram (Fig. 9B). By late Turonian or Coniacian time, Hornbrook sediment sources had shifted into the Late Cretaceous Sierra Nevada batholith and possibly Idaho batholith, resulting in widespread sedimentation throughout the Hornbrook region that was characterized by abundant Late Cretaceous detrital zircons with variable ε_{Hf} values, scarce Early Cretaceous grains, and a broad distribution of Jurassic grains (middle group of Fig. 4, including the Ditch Creek Siltstone in the Cottonwood Creek valley, Barneburg Hill, and the Suncrest Road Quarry sample). These samples contain small but variable amounts of pre-Mesozoic detrital zircon (2%–13%) and also plot near island-arc andesite, but relatively closer to North American shale composite and upper continental crust than the older samples (Fig. 9B). Following the Coniacian pulse of Late Cretaceous detrital zircon, upper Hornbrook strata (upper group of Fig. 4, including the Rocky Gulch Sandstone and Blue Gulch Mudstone) continued to receive Late Cretaceous detrital zircon, but also abundant Early Cretaceous zircon (125–100 Ma), and variable abundance of Early and Middle–Late Jurassic detrital zircon (Figs. 3 and 4). These upper samples contain up to 19% pre-Mesozoic detrital zircon and plot closer to the North American shale composite and upper continental crust values on a La-Th-Sc ternary diagram (Fig. 9B).

Tectonic Implications

Sharman et al. (2015) suggested that a Cenomanian–Coniacian drainage divide along the axis of the Cretaceous Cordilleran arc precluded westward transport of 100–85 Ma zircon into the forearc region, and results presented here suggest that much of the detritus eroded from the Late Cretaceous rocks of the Sierran Crest intrusive suite and/or coeval plutons in the northern Sierra Nevada may have been transported northward and westward into the Hornbrook basin beginning as early as late Turonian time (ca. 90 Ma; Fig. 11).

DeCelles (2004) suggested that shortening in the Sevier thrust belt led to crustal thicknesses of 50–60 km and development of an elevated Nevadaplano in conjunction with voluminous mid- to Late Cretaceous magmatism in the Sierra Nevada batholith. Paleoelevation studies by Mulch et al. (2006) and Cassel et al. (2009) concluded that the Sierra Nevada uplift occurred in Late Cretaceous or early Cenozoic time, and continuity of Eocene paleodrainage systems suggests that the Sierra Nevada formed the western flank of the Nevadaplano (e.g., Faulds et al., 2005; Henry, 2009). Snell et al. (2014) used carbonate isotope thermometry to suggest that the Nevadaplano stood at ≥2 km elevation during the latest Cretaceous. Bonde et al. (2014) compared vertebrate fauna in Early and Late Cretaceous units of east-central Nevada to show that regional uplift of the Nevadaplano was entirely a Late Cretaceous event, and it may have reached its maximum during Maastrichtian time. Thermo-

chronology of the northern Sierra Nevada indicates exhumation and erosional denudation of the region from 90 to 60 Ma, as a result of earlier orogenic thickening of the crust and emplacement of the Late Cretaceous batholith (Cecil et al., 2006). Resulting sediment derived from eroded arc rocks may have been transported northward along the axis of the arc, between the western drainage divide along the arc crest and the rising Nevadaplano to the east (Fig. 11).

The abrupt appearance of abundant 100–85 Ma detrital zircons in the detrital age signatures of Coniacian Hornbrook strata, even extending onto the Klamath Mountains at the Suncrest Road Quarry, suggests that regional uplift of the Sierran arc and Nevadaplano began during Coniacian time. Late Cretaceous detrital zircons persist in the Hornbrook samples through Maastrichtian deposition, but they are relatively less abundant in the detrital age signatures, with additional contribution of more Early Cretaceous and Jurassic detrital zircons (Figs. 3 and 4). This broadening of the detrital zircon age signature may reflect increased catchment size as fluvial systems eroded east- and southeastward into the elevated Nevadaplano and the Sierran arc rocks that formed its western flank. In addition, the gradual increase in 100–85 Ma zircons in the Santonian to Paleogene Great Valley forearc, concomitant with the relative decrease of this Late Cretaceous age peak in the Hornbrook region, may have resulted from breaching of the western drainage divide within the arc and ensuing westward transport of sediment eroded from Late Cretaceous plutons of the eastern Sierra Nevada (e.g., Sharman et al., 2015). The presence of the elevated Nevadaplano during the Late Cretaceous (DeCelles, 2004; Snell et al., 2014) meant that relatively little arc-derived detritus was shed to the east, and even less crossed the Nevadaplano into the foreland basin (Dickinson et al., 2012; Sharman et al., 2015).

It is possible that Jurassic and Early Cretaceous sediment present throughout the Hornbrook strata was derived from the Klamath Mountains and/or the Blue Mountains, but the presence of Late Cretaceous deposition on the Klamath Mountains at the Suncrest Road Quarry (Fig. 2), 80 km west of Hornbrook Formation outcrops, and Late Cretaceous deep-water deposition on the Blue Mountains in the Ochoco basin (e.g., Dickinson, 1979; Kleinhans et al., 1984; Dorsey and Lenegan, 2007) suggest that these regions were the locus of subsidence and sedimentation, rather than erosion, during the Late Cretaceous. Thus, the limited outcrop extent of the Hornbrook Formation may represent only a sliver of a much larger Late Cretaceous Hornbrook basin (Fig. 11). Subsidence of the Hornbrook region may have been in part a response to Late Cretaceous uplift of the early Idaho batholith (e.g., Giorgis et al., 2008), northern Sierra Nevada (e.g., Cecil et al., 2006), and Nevadaplano (e.g., DeCelles, 2004; Snell et al., 2014).

Improved Record of Episodic Magmatism

Unlike bedrock analyses, detrital zircon ages are unlikely to reflect sampling of a single pluton or isolated part of an arc, but rather they provide an averaged long-term history of arc magmatism (e.g., de Silva et al., 2015). A comparison of large data sets of bedrock and detrital zircons from the Sierra Nevada arc demonstrates that the detrital zircon record accurately reflects the timing of magmatic flare-ups and lulls in the Sierran arc, but it provides a poor proxy for estimating the volume of magmatic addition during each flare-up event (Paterson and Ducea, 2015). Sedimentary successions are unlikely to accurately reflect the volume of magmatic flare-up events because they may include nonarc sources and may over- or underrepresent magmatic arc age distributions, depending on zircon fertility of sources (e.g., Moecher and Samson, 2006), catchment size (e.g., Ingersoll, 1990), and depositional age. However, closer approximation of the timing, duration, and volume of magmatic flare-up events also depends on thorough sampling of arc-derived strata. Intra-arc drainage systems may have transported a significant volume of sediment eroded from Late Cretaceous Sierran plutons northward into the Hornbrook region, rather than westward into the Great Valley forearc or eastward into the retroarc region. Detrital zircon ages from the forearc and retroarc regions would therefore underrepresent the Late Cretaceous magmatic flare-up event. This potential for sediment transport to depocenters not directly linked to present-day arc exposures is critical to recognize so that the detrital zircon record forms a detailed record of magmatic activity, providing a powerful, and necessary, complement to bedrock geochronology.

CONCLUSIONS

Deposition in the Hornbrook basin may have begun as early as Albian time (e.g., Surpless and Beverly, 2013), but most of the Hornbrook strata were deposited during the Late Cretaceous, and provenance results presented here suggest that the Hornbrook region received abundant sediment derived from the Late Cretaceous Sierra Nevada batholith and possibly the early magmatic phase of the Idaho batholith beginning in Coniacian time. The Coniacian influx of Late Cretaceous detrital zircon into the Hornbrook region may signal the rise of the Nevadaplano and the Sierran arc rocks that formed its western flank, as well as erosion of rapidly exhumed rocks in the western Idaho shear zone. Uplift of the Sierran arc and Nevadaplano from overthickening of the crust and emplacement of voluminous Late Cretaceous magmatism in the Sierran arc, combined with transpressive uplift along the western Idaho shear zone, may have led to subsidence in the greater Hornbrook region, resulting in more widespread Late Cretaceous deposition than modern outcrop extent suggests. Sediment was transported north-, northwest-, and westward into the subsiding Hornbrook region by fluvial systems draining the rising Sierran arc and Idaho batholith during the early Late Cretaceous, with catchments increasing as fluvial systems reached further east and south with time. Thus, the sedimentary record of the Late Cretaceous magmatic flare-up event in the northern Sierran arc may be best documented in the Hornbrook basin northwest of the arc, rather than either the forearc or retroarc systems that flank the Sierra Nevada.

ACKNOWLEDGMENTS

I thank Charles Knaack, Laureen Wagoner, and Richard Conrey at the GeoAnalytical Laboratory at Washington State University for geochemical analyses. Detrital zircon ages newly presented here were collected at the University of Arizona LaserChron Center with assistance from Nicky Geissler and Mark Pecha, and I gratefully acknowledge National Science Foundation (NSF) grant EAR-1032156 for support of the Arizona LaserChron Center. I thank Jad D'Allura, Heath Hopson, Nicholis Candusso, and Travis Dodson for invaluable assistance in sample collection and processing, as well as with detrital zircon age data collection. Scott Paterson, an anonymous reviewer, and Associate Editor Todd LaMaskin provided helpful reviews. This research was funded by NSF EAR ICER 846695.

REFERENCES CITED

Anderson, B.S., Schwartz, J.J., Johnson, K., Wooden, J.L., and Mueller, P.A., 2011, U-Pb geochronology and Hf isotope geochemistry of the Mountain Home metamorphic complex, Blue Mountains Province, northeastern Oregon: Geological Society of America Abstracts with Programs, v. 43, no. 4, p. 76.

Barth, A.P., Wooden, J.L., Jacobsen, C.E., and Probst, K., 2004, U-Pb geochronology and geochemistry of the McCoy Mountains Formation, southeastern California: A Cretaceous retro-arc foreland basin: Geological Society of America Bulletin, v. 116, p. 142–153, doi:10.1130/B25288.1.

Barth, A.P., Wooden, J.L., Jacobson, C.E., and Economos, R.C., 2013, Detrital zircon as a proxy for tracking the magmatic arc system: The California arc example: Geology, v. 41, p. 223–226, doi:10.1130/G33619.1.

Barton, M.D., Battles, D.A., Debout, G.E., Capo, R.C., Christensen, J.N., Davis, S.R., Hanson, R.B., Michelsen, C.J., and Trim, H.E., 1988, Mesozoic contact metamorphism in the western United States, *in* Ernst, W.G., ed., Metamorphism and Crustal Evolution of the Western United States, Rubey Volume 7: Englewood Cliffs, New Jersey, Prentice-Hall, p. 110–178.

Bateman, P.C., 1992, Plutonism in the Central Part of the Sierra Nevada Batholith, California: U.S. Geological Survey Professional Paper 1483, 186 p.

Batt, G.E., Cashman, S.M., Garver, J.I., and Bigelow, J.J., 2010, Thermotectonic evidence for two-stage extension on the Trinity detachment surface, eastern Klamath Mountains, California: American Journal of Science, v. 310, p. 261–281, doi:10.2475/04.2010.02.

Benford, B., Crowley, J., Schmitz, M., Northrup, C.J., and Tikoff, B., 2010, Mesozoic magmatism and deformation in the northern Owyhee Mountains, Idaho: Implications for along-zone variations for the western Idaho shear zone: Lithosphere, v. 2, p. 93–118, doi:10.1130/L76.1.

Bhatia, M.R., and Crook, K.A.W., 1986, Trace element characteristics of graywackes and tectonic setting discrimination of sedimentary basins: Contributions to Mineralogy and Petrology, v. 92, p. 181–193, doi:10.1007/BF00375292.

Bonde, J.W., Druschke, P.A., and Hilton, R.P., 2014, Paleogeography and uplift history of the Sevier retroarc hinterland: What say the critters?: Geological Society of America Abstracts with Programs, v. 46, no. 5, p. 26.

Cao, W., Paterson, S., Memeti, V., Mundil, R., Anderson, J.L., and Schmidt, K., 2015, Tracking paleodeformation fields in the Mesozoic central Sierra Nevada arc: Implications for intra-arc cyclic deformation and arc tempos: Lithosphere, v. 7, no. 3, p. 296–320, doi:10.1130/L389.1.

Cassel, E.J., Graham, S.A., and Chamberlain, C.P., 2009, Cenozoic tectonic and topographic evolution of the northern Sierra Nevada, California, through stable isotope paleoaltimetry in volcanic glass: Geology, v. 37, p. 547–550, doi:10.1130/G25572A.1.

Cecil, M.R., Ducea, M.N., Reiners, P.W., and Chase, C.G., 2006, Cenozoic exhumation of the northern Sierra Nevada, California, from (U-Th)/He thermochronology: Geological Society of America Bulletin, v. 118, p. 1481–1488, doi:10.1130/B25876.1.

Cecil, M.R., Gehrels, G.E., Ducea, M.N., and Patchett, J., 2011, U-Pb-Hf characterization of the central Coast Mountains batholith: Implications for petrogenesis and crustal architecture: Lithosphere, v. 3, p. 247–260, doi:10.1130/L134.1.

Cecil, M.R., Rotberg, G.L., Ducea, M.N., Saleeby, J.B., and Gehrels, G.E., 2012, Magmatic growth and batholithic root development in the northern Sierra Nevada, California: Geosphere, v. 8, p. 592–606, doi:10.1130/GES00729.1.

Chen, J.H., and Moore, J.G., 1982, Uranium-lead isotopic ages from the Sierra Nevada batholith, California: Journal of Geophysical Research, v. 87, p. 4761–4784, doi:10.1029/JB087iB06p04761.

Coleman, D.S., and Glazner, A.F., 1997, The Sierra Crest magmatic event: Rapid formation of juvenile crust during the Late Cretaceous in California: International Geology Review, v. 39, p. 768–787, doi:10.1080/00206819709465302.

Constenius, K.N., Johnson, R.A., Dickinson, W.R., and Williams, T.A., 2000, Tectonic evolution of the Jurassic–Cretaceous Great Valley forearc, California: Implications for the Franciscan thrust-wedge hypothesis: Geological Society of America Bulletin, v. 112, p. 1703–1723, doi:10.1130/0016-7606(2000)112<1703:TEOTJC>2.0.CO;2.

Cowan, D.S., Brandon, M.T., and Garver, J.I., 1997, Geologic tests of hypotheses for large coastwise displacements—A critique illustrated by the Baja–British Columbia controversy: American Journal of Science, v. 297, p. 117–173, doi:10.2475/ajs.297.2.117.

Cumming, G.L., and Richards, J.R., 1975, Ore lead isotope ratios in a continuously changing Earth: Earth and Planetary Science Letters, v. 28, p. 155–171, doi:10.1016/0012-821X(75)90223-X.

DeCelles, P.G., 2004, Late Jurassic to Eocene evolution of the Cordilleran thrust belt and foreland basin system, western U.S.A.: American Journal of Science, v. 304, p. 105–168, doi:10.2475/ajs.304.2.105.

DeGraaff-Surpless, K., Graham, S.A., Wooden, J.L., and McWilliams, M.O., 2002, Detrital zircon provenance analysis of the Great Valley Group, California: Evolution of an arc-forearc system: Geological Society of America Bulletin, v. 114, p. 1564–1580, doi:10.1130/0016-7606(2002)114<1564:DZPAOT>2.0.CO;2.

DeGraaff-Surpless, K., Mahoney, J.B., Wooden, J.L., and McWilliams, M.O., 2003, Lithofacies control in detrital zircon provenance studies: Insights from the Cretaceous Methow Basin: Geological Society of America Bulletin, v. 115, no. 8, p. 899–915.

DePaolo, D.J., 1981, A neodymium and strontium isotopic study of the Mesozoic calc-alkaline granitic batholiths of the Sierra Nevada and Peninsular Ranges, California: Journal of Geophysical Research, v. 86, p. 10,470–10,488, doi:10.1029/JB086iB11p10470.

de Silva, S.L., Riggs, N.R., and Barth, A.P., 2015, Quickening the pulse: Fractal tempos in continental arc magmatism: Elements, v. 11, p. 113–118, doi:10.2113/gselements.11.2.113.

Dickinson, W.R., 1979, Mesozoic forearc basin in central Oregon: Geology, v. 7, p. 166–170, doi:10.1130/0091-7613(1979)7<166:MFBICO>2.0.CO;2.

Dickinson, W.R., and Gehrels, G.E., 2008, Sediment delivery to the Cordilleran foreland basin: Insights from U-Pb ages of detrital zircons in Upper Jurassic and Cretaceous strata of the Colorado Plateau: American Journal of Science, v. 308, p. 1041–1082, doi:10.2475/10.2008.01.

Dickinson, W.R., and Gehrels, G.E., 2009, Use of U-Pb ages of detrital zircons to infer maximum depositional ages of strata: A test against a Colorado Plateau Mesozoic database: Earth and Planetary Science Letters, v. 288, p. 115–125, doi:10.1016/j.epsl.2009.09.013.

Dickinson, W.R., and Thayer, T.P., 1978, Paleogeographic and paleotectonic implications of Mesozoic stratigraphy and structure in the John Day inlier of central Oregon, *in* Howell, D.G., and McDougall, K.A., eds., Mesozoic Paleogeography of the Western United States: Los Angeles, Pacific Section, Society of Economic Paleontologists and Mineralogists, Paleogeography Symposium 2, p. 147–161.

Dickinson, W.R., Beard, S.L., Brakenridge, G.R., Erjavec, J.L., Ferguson, R.C., Inman, K.F., Knepp, R.A., Lindberg, F.A., and Ryberg, P.T., 1983, Provenance of North American Phanerozoic sandstones in relation to tectonic setting: Geological Society of America Bulletin, v. 94, p. 222–235, doi:10.1130/0016-7606(1983)94<222:PONAPS>2.0.CO;2.

Dickinson, W.R., Lawton, T.F., Pecha, M., Davis, S.J., Gehrels, G.E., and Young, G.A., 2012, Provenance of the Paleogene Colton Formation (Uinta Basin) and Cretaceous–Paleogene provenance evolution in the Utah foreland: Evidence from U-Pb ages of detrital zircons, paleocurrent trends, and sandstone petrofacies: Geosphere, v. 8, p. 854–880, doi:10.1130/GES00763.1.

Dorsey, R.J., and LaMaskin, T.A., 2007, Stratigraphic record of Triassic-Jurassic collisional tectonics in the Blue Mountains Province, northeastern Oregon: American Journal of Science, v. 307, p. 1167–1193, doi:10.2475/10.2007.03.

Dorsey, R.J., and Lenegan, R.J., 2007, Structural controls on middle Cretaceous sedimentation in the Toney Butte area, Ochoco basin, central Oregon, *in* Cloos, M., ed., Convergent Margin Terranes and Associated Regions: Geological Society of America Special Paper 419, p. 97–115.

Ducea, M., 2001, The California arc: Thick granitic batholiths, eclogitic residues, lithospheric-scale thrusting, and magmatic flare-ups: GSA Today, v. 11, p. 4–10, doi:10.1130/1052-5173(2001)011<0004:TCATGB>2.0.CO;2.

Ducea, M., and Barton, M.D., 2007, Igniting flare-up events in Cordilleran arcs: Geology, v. 35, p. 1047–1050, doi:10.1130/G23898A.1.

Ducea, M.N., Paterson, S.R., and DeCelles, P.G., 2015, High-volume magmatic events in subduction systems: Elements, v. 11, p. 99–104, doi:10.2113/gselements.11.2.99.

Elliott, M.A., 1971, Stratigraphy and Petrology of the Late Cretaceous Rocks near Hilt and Hornbrook, Siskiyou County, California, and Jackson County, Oregon [Ph.D. dissertation]: Corvallis, Oregon, Oregon State University, 171 p.

Ernst, W.G., 2013, Earliest Cretaceous Pacificward offset of the Klamath Mountains Salient, NW California–SW Oregon: Lithosphere, v. 5, p. 151–159, doi:10.1130/L247.1.
Ernst, W.G., Snow, C.A., and Scherer, H.H., 2008, Contrasting early and late Mesozoic petrotectonic evolution of northern California: Geologic Society of America Bulletin, v. 120, no. 1–2, p. 179–194.
Faulds, J.E., Henry, C.D., and Hinz, N.H., 2005, Kinematics of the northern Walker Lane: An incipient transform fault along the Pacific–North American plate boundary: Geology, v. 33, p. 505–508, doi:10.1130/G21274.1.
Fralick, P.W., 2003, Geochemistry of clastic sedimentary rocks: Ratio techniques, *in* Lentz, D.R., ed., Geochemistry of Sediments and Sedimentary Rocks: Evolutionary Considerations to Mineral Deposit–Forming Environments: Geological Association of Canada GeoText 4, p. 85–103.
Gaschnig, R.M., Vervoort, J.D., Lewis, R.S., and McClelland, W.C., 2010, Migrating magmatism in the northern US Cordillera: In situ U-Pb geochronology of the Idaho batholith: Contributions to Mineralogy and Petrology, v. 159, p. 863–883, doi:10.1007/s00410-009-0459-5.
Gaschnig, R.M., Vervoort, J., Lewis, R.S., and Tikoff, B., 2011, Isotopic evolution of the Idaho batholith and Challis intrusive province, northern US Cordillera: Journal of Petrology, v. 52, p. 2397–2429, doi:10.1093/petrology/egr050.
Gehrels, G.E., 2012, Detrital zircon U-Pb geochronology: Current methods and new opportunities, *in* Busby, C., and Azor, A., eds., Tectonics of Sedimentary Basins: Recent Advances: Chichester, UK, John Wiley & Sons, Ltd., p. 47–62.
Gehrels, G., 2014, Detrital zircon U-Pb geochronology applied to tectonics: Annual Review of Earth and Planetary Sciences, v. 42, p. 127–149, doi:10.1146/annurev-earth-050212-124012.
Gehrels, G., and Pecha, M., 2014, Detrital zircon geochronology and Hf isotope geochemistry of Paleozoic and Triassic passive margin strata of western North America: Geosphere, v. 10, p. 49–65.
Gehrels, G.E., Valencia, V., and Pullen, A., 2006, Detrital zircon geochronology by laser-ablation multicollector ICPMS at the Arizona LaserChron Center, *in* Olszewski, T., ed., Geochronology: Emerging Opportunities: The Paleontological Society Papers, v. 12, p. 67–76.
Giorgis, S., McClelland, W., Fayon, A., Singer, B.S., and Tikoff, B., 2008, Timing of deformation and exhumation in the western Idaho shear zone, McCall, Idaho: Geological Society of America Bulletin, v. 120, p. 1119–1133, doi:10.1130/B26291.1.
Golia, R.T., and Nilsen, T.H., 1984, Sandstone petrography of the Upper Cretaceous Hornbrook Formation, Oregon and California, *in* Nilsen, T.H., ed., Geology of the Upper Cretaceous Hornbrook Formation, Oregon and California: Los Angeles, Pacific Section, Society of Economic Paleontologists and Mineralogists, Book 42, p. 99–109.
Grasse, S.W., Gehrels, G.E., Lahren, M.M., Schweickert, R.A., and Barth, A.P., 2001, U-Pb geochronology of detrital zircons from the Snow Lake pendant, central Sierra Nevada—Implications for Late Jurassic–Early Cretaceous dextral strike-slip faulting: Geology, v. 29, p. 307–310, doi:10.1130/0091-7613(2001)029<0307:UPGODZ>2.0.CO;2.
Gromet, L.P., Dymek, R.F., Haskin, L.A., and Korotev, R.L., 1984, The "North American shale composite": Its compilation, major and trace element characteristics: Geochimica et Cosmochimica Acta, v. 48, p. 2469–2482, doi:10.1016/0016-7037(84)90298-9.
Henry, C.D., 2009, Uplift of the Sierra Nevada, California: Geology, v. 37, p. 575–576, doi:10.1130/focus062009.1.
Housen, B.A., and Dorsey, R.J., 2002, Tectonic significance of paleomagnetic results from the Ochoco and Hornbrook basins, Oregon: Geological Society of America Abstracts with Programs, v. 34, no. 5, p. 103.
Imlay, R.W., Dole, H.M., Wells, F.G., and Peck, D.L., 1959, Relations of certain Jurassic and Lower Cretaceous formations in southwestern Oregon: American Association of Petroleum Geologists Bulletin, v. 43, p. 2770–2785.
Ingersoll, R.V., 1990, Actualistic sandstone petrofacies: Discriminating modern and ancient source rocks: Geology, v. 18, p. 733–736, doi:10.1130/0091-7613(1990)018<0733:ASPDMA>2.3.CO;2.
Irwin, W.P., 1960, Geologic Reconnaissance of the Northern Coast Ranges and Klamath Mountains, California, with a Summary of the Mineral Resources: California Division of Mines Bulletin 179, 80 p.
Irwin, W.P., 2003, Correlation of the Klamath Mountains and Sierra Nevada: U.S. Geological Survey Open-File Report 02–490, scale 1:1,000,000.
Jameossanaie, A., and Lindsley-Griffin, N., 1993, Palynology and plate tectonics: A case study on Cretaceous terrestrial sediments in the eastern Klamath Mountains of northern California, USA: Palynology, v. 17, p. 11–45, doi:10.1080/01916122.1993.9989417.
Johnson, D.M., Hooper, P.R., and Conrey, R.M., 1999, XRF analysis of rocks and minerals for major and trace elements on a single low dilution Li-tetraborate fused bead: Advances in X-Ray Analysis, v. 41, p. 843–867.
Jones, D.L., 1959, Stratigraphy of Upper Cretaceous rocks in the Yreka-Hornbrook area, northern California: Geological Society of America Bulletin, v. 70, p. 1726–1727.
Jones, D.L., and Irwin, W.P., 1971, Structural implications of an offset Early Cretaceous shoreline in northern California: Geological Society of America Bulletin, v. 82, p. 815–822, doi:10.1130/0016-7606(1971)82[815:SIOAOE]2.0.CO;2.
Kleinhans, L.C., Balcells-Baldwin, E.A., and Jones, R.E., 1984, A paleogeographic reinterpretation of some middle Cretaceous units, north-central Oregon: Evidence for a submarine turbidite system, *in* Nilsen, T.H., ed., Geology of the Upper Cretaceous Hornbrook Formation, Oregon and California: Los Angeles, Pacific Section, Society of Economic Paleontologists and Mineralogists, Book 42, p. 239–257.
Knaack, C., Cornelius, S.B., and Hooper, P.R., 1994, Trace Element Analyses of Rocks and Minerals by ICP-MS (last updated 1994): http://www.sees.wsu.edu/Geolab/note/icpms.html. (accessed September 2014).
Lackey, J.S., Cecil, M.R., Windham, C.J., Frazer, R.E., Bindeman, I.N., and Gehrels, G.E., 2012, The Fine Gold intrusive suite: The roles of basement terranes and magma source development in the Early Cretaceous Sierra Nevada batholith: Geosphere, v. 8, p. 292–313, doi:10.1130/GES00745.1.
LaMaskin, T.A., Dorsey, R.J., and Vervoort, J.D., 2008, Tectonic controls on mudrock geochemistry, Mesozoic rocks of eastern Oregon and western Idaho, U.S.A.: Implications for Cordilleran tectonics: Journal of Sedimentary Research, v. 78, p. 765–783, doi:10.2110/jsr.2008.087.
LaMaskin, T.A., Vervoort, J.D., Dorsey, R.J., and Wright, J.E., 2011, Early Mesozoic paleogeography and tectonic evolution of the western United States; insights from detrital zircon U-Pb geochronology, Blue Mountains Province, northeastern Oregon: Geological Society of America Bulletin, v. 123, p. 1939–1965, doi:10.1130/B30260.1.
Lerch, D.W., Klemperer, S.L., Glen, J.M.G., Ponce, D.A., and Miller, E.L., 2007, Crustal structure of the northwestern Basin and Range Province and its transition to unextended volcanic plateaus: Geochemistry, Geophysics, Geosystems, v. 8, Q02011, doi:10.1029/2006GC001429.
Lewis, R.S., Kiilsgaard, T.H., Bennett, E.H., and Hall, W.E., 1987, Lithologic and chemical characteristics of the central and southeastern part of the southern lobe of the Idaho batholith, *in* Vallier, T.L., and Brooks, H.C., eds., Geology of the Blue Mountains Region of Oregon, Idaho, and Washington; the Idaho Batholith and its Border Zone: U.S. Geological Survey Professional Paper 1436, p. 171–196.
Ludwig, K.R., 2011, Isoplot 4.15: http://www.bgc.org/isoplot_etc/isoplot.html (accessed November 2012).
Mankinen, E.A., and Irwin, W.P., 1982, Paleomagnetic study of some Cretaceous and Tertiary sedimentary rocks of the Klamath Mountains province, California: Geology, v. 10, p. 82–87, doi:10.1130/0091-7613(1982)10<82:PSOSCA>2.0.CO;2.
McKnight, B.K., 1971, Petrology and Sedimentation of Cretaceous and Eocene Rocks in the Medford-Ashland Region, Southwestern Oregon [Ph.D. dissertation]: Corvallis, Oregon, Oregon State University, 177 p.
McLennan, S.M., 1989, Rare earth elements in sedimentary rocks: Influence on provenance and sedimentary processes, *in* Lipin, B.R., and McKay, G.A., eds., Geochemistry and Mineralogy of Rare Earth Elements: Reviews in Mineralogy, v. 21, p. 169–200.
McLennan, S.M., Taylor, S.R., McCulloch, M.T., and Maynard, J.B., 1990, Geochemical and Nd-Sr isotopic composition of deep-sea turbidites; crustal evolution and plate tectonic associations: Geochimica et Cosmochimica Acta, v. 54, p. 2015–2050, doi:10.1016/0016-7037(90)90269-Q.
McLennan, S.M., Hemming, S., McDaniel, D.K., and Hanson, G.N., 1993, Geochemical approaches to sedimentation, provenance, and tectonics, *in* Johnson, M.J., and Basu, A., eds., Processes Controlling the Composition of Clastic Sediments: Geological Society of America Special Paper 284, p. 21–40.
Memeti, V., Gehrels, G.E., Paterson, S.R., Thompson, J.M., Mueller, R.M., and Pignotta, G.S., 2010, Evaluating the Mojave–Snow Lake fault hypothesis and origins of central Sierran metasedimentary pendant strata using detrital zircon provenance analysis: Lithosphere, v. 2, p. 341–360, doi:10.1130/L58.1.
Miller, D.M., Nilsen, T.H., and Bilodeau, W.L., 1992, Late Cretaceous to early Eocene geologic evolution of the U.S. Cordillera, *in* Burchfiel, B.C., Lipman, P.W., and Zoback, M.L., eds., The Cordilleran Orogen: Conterminous U.S.: Boulder, Colorado, The Geological Society of America, The Geology of North America, v. G-3, p. 205–260.

Moecher, D.P., and Samson, S.D., 2006, Differential zircon fertility of source terranes and natural bias in the detrital zircon record: Implications for sedimentary provenance analysis: Earth and Planetary Science Letters, v. 247, p. 252–266, doi:10.1016/j.epsl.2006.04.035.

Mongelli, G., Critelli, S., Perri, F., Sonnino, M., and Perrone, V., 2006, Sedimentary recycling, provenance and paleoweathering from chemistry and mineralogy of Mesozoic continental redbed mudrocks, Peloritani Mountains, southern Italy: Geochemical Journal, v. 40, p. 197–209, doi:10.2343/geochemj.40.197.

Mulch, A., Graham, S.A., and Chamberlain, C.P., 2006, Hydrogen isotopes in Eocene river gravels and paleoelevation of the Sierra Nevada: Science, v. 313, p. 87–89, doi:10.1126/science.1125986.

Nesbitt, H.W., and Young, G.M., 1982, Early Proterozoic climates and plate motions inferred from major element chemistry of lutites: Nature, v. 299, p. 715–717, doi:10.1038/299715a0.

Nesbitt, H.W., and Young, G.M., 1984, Prediction of some weathering trends of plutonic and volcanic rocks based on thermodynamic and kinetic considerations: Geochimica et Cosmochimica Acta, v. 48, p. 1523–1534, doi:10.1016/0016-7037(84)90408-3.

Nesbitt, H.W., and Young, G.M., 1989, Formation and diagenesis of weathering profiles: The Journal of Geology, v. 97, p. 129–147, doi:10.1086/629290.

Nilsen, T.H., 1984, Stratigraphy, sedimentology, and tectonic framework of the Upper Cretaceous Hornbrook Formation, Oregon and California, *in* Nilsen, T.H., ed., Geology of the Upper Cretaceous Hornbrook Formation, Oregon and California: Los Angeles, Pacific Section, Society of Economic Paleontologists and Mineralogists, Book 42, p. 51–88.

Nilsen, T.H., 1993, Stratigraphy of the Cretaceous Hornbrook Formation, Southern Oregon and Northern California: U.S. Geological Survey Professional Paper 1521, 89 p.

Northrup, C.J., Schmitz, M., Kurz, G., and Tumpane, K., 2011, Tectonomagmatic evolution of distinct arc terranes in the Blue Mountains Province, Oregon and Idaho, *in* Lee, J., and Evans, J.P., eds., Geologic Field Trips to the Basin and Range, Rocky Mountains, Snake River Plain, and Terranes of the U.S. Cordillera: Geological Society of America Field Guide 21, p. 67–88.

Oles, K.F., and Enlows, H.E., 1971, Bedrock Geology of the Mitchell Quadrangle, Wheeler County, Oregon: State of Oregon Department of Geology and Mineral Resources Bulletin 72, 62 p.

Paterson, S.R., and Ducea, M.N., 2015, Arc magmatic tempos: Gathering the evidence: Elements, v. 11, p. 91–98, doi:10.2113/gselements.11.2.91.

Paterson, S.R., Okaya, D., Memeti, V., Economos, R., and Miller, R.B., 2011, Magma addition and flux calculations of incrementally constructed magma chambers in continental margin arcs: Combined field, geochronologic, and thermal modeling studies: Geosphere, v. 7, p. 1439–1468, doi:10.1130/GES00696.1.

Peck, D.L., Imlay, R.W., and Popenoe, W.P., 1956, Upper Cretaceous rocks of parts of southwestern Oregon and northern California: American Association of Petroleum Geologists Bulletin, v. 40, p. 1968–1984.

Ryan, K.M., and Williams, D.M., 2007, Testing the reliability of discrimination diagrams for determining the tectonic depositional environment of ancient sedimentary basins: Chemical Geology, v. 242, p. 103–125, doi:10.1016/j.chemgeo.2007.03.013.

Schwartz, J.J., Snoke, A.W., Cordrey, F., Johnson, K., Frost, C.D., Barnes, C.G., LaMaskin, T.A., and Wooden, J.L., 2011, Late Jurassic magmatism, metamorphism, and deformation in the Blue Mountains Province, northeast Oregon: Geological Society of America Bulletin, v. 123, p. 2083–2111, doi:10.1130/B30327.1.

Sharman, G.R., Graham, S.A., Grove, M., Kimbrough, D.L., and Wright, J.E., 2015, Detrital zircon provenance of Late Cretaceous–Eocene California forearc: Influence of Laramide low-angle subduction on sediment dispersal and paleogeography: Geological Society of America Bulletin, v. 127, p. 38–60, doi:10.1130/B31065.1.

Snell, K.E., Koch, P.L., Druschke, P., Foreman, B.Z., and Eiler, J.M., 2014, High elevation of the 'Nevadaplano' during the Late Cretaceous: Earth and Planetary Science Letters, v. 386, p. 52–63, doi:10.1016/j.epsl.2013.10.046.

Snow, C.A., and Scherer, H., 2006, Terranes of the western Sierra Nevada foothills metamorphic belt, California; a critical review: International Geology Review, v. 48, p. 46–62, doi:10.2747/0020-6814.48.1.46.

Sun, S.S., and McDonough, W.F., 1989, Chemical and isotopic systematic of oceanic basalts: Implications for mantle composition and processes, *in* Saunders, A.D., and Norry, M.J., eds., Magmatism in Ocean Basins: Geological Society, London, Special Publication 42, p. 313–345.

Surpless, K.D., and Beverly, E.M., 2013, Understanding a critical basinal link in Cretaceous Cordilleran paleogeography: Detailed provenance of the Hornbrook Formation, Oregon and California: Geological Society of America Bulletin, v. 125, p. 709–727, doi:10.1130/B30690.1.

Taylor, S.R., and McLennan, S.M., 1985, The Continental Crust: Its Composition and Evolution: Oxford, U.K., Blackwell, 312 p.

Todt, M.K., Surpless, K.D., and Shaw, B.R.G., 2011, Testing the utility of detrital zircon hafnium signatures for sedimentary provenance in the northern Great Valley Group, California: Geological Society of America Abstracts with Programs, v. 43, no. 4, p. 68.

Van Buer, N.J., and Miller, E.L., 2010, Sahwave batholith, NW Nevada: Cretaceous arc flare-up in a basinal terrane: Lithosphere, v. 2, p. 423–446, doi:10.1130/L105.1.

Van Buer, N.J., Miller, E.L., and Dumitru, T.A., 2009, Early Tertiary paleogeologic map of the northern Sierra Nevada batholith and the northwestern Basin and Range: Geology, v. 37, p. 371–374, doi:10.1130/G25448A.1.

Walker, G.W., and McLeod, N.S., 1991, Geologic Map of Oregon: U.S. Geological Survey, scale 1:500,000, 2 sheets.

Walker, J.D., Geissman, J.W., Bowring, S.A., and Babcock, L.E., compilers, 2012, Geologic Time Scale v. 4.0: Boulder, Colorado, Geological Society of America, doi:10.1130/2012.CTS004R3C.

Walker, N.W., 1995, Tectonic Implications of U-Pb Zircon Ages of the Canyon Mountain Complex, Sparta Complex, and Related Metaplutonic Rocks of the Baker Terrane, Northeastern Oregon: U.S. Geological Survey Professional Paper 1438, p. 247–269.

Wiley, T.J., McClaughry, J.D., and D'Allura, J.A., 2011, Geologic Database and Generalized Geologic Map of Bear Creek Valley, Jackson County, Oregon: Oregon Department of Geology and Mineral Industries Open-File Report O-2011-11, scale 1:24,000.

Wyld, S.J., Umhoefer, P.J., and Wright, J.E., 2006, Reconstructing northern Cordilleran terranes along known Cretaceous and Cenozoic strike-slip faults: Implications for the Baja–British Columbia hypothesis and other models, *in* Haggart, J.W., Enkin, R.J., and Monger, J.W.H., eds., Paleogeography of the North American Cordillera: Evidence For and Against Large-Scale Displacements: Geological Association of Canada Special Paper 46, p. 277–298.